# V. Potential Future Conditions of the Colorado Plateau

Predicting potential future conditions for the Colorado Plateau was approached in several ways that relied heavily on fuzzy logic modeling for near-term development, potential energy development, near-term terrestrial landscape and aquatic intactness, and potential mid-century (2060) climate change impacts. Results for each analysis were then assessed against the distribution of each of the conservation elements to illustrate their potential future status. Lack of source data for future projections was a common issue resulting in underestimates of what is likely to occur, including in the near-term 2025 time frame. Maximum potential (or long term) energy development has an indeterminate time frame; it is based on broad scale polygons representing energy zones rather than specific leases or applications. For this reason, maximum potential energy development, as discussed in Section 5.2, when overlaid on conservation elements' distributions may overestimate the impacts to species, habitats, and sites. The potential energy development analysis considered all potential known traditional (Copeland et al. 2009) and renewable energy projections. Projecting into the future is a challenging endeavor and the results should be viewed critically as they possess many uncertainties; they should not be relied upon for detailed site-level planning and management without additional information and analysis. The results do provide one view of what to expect for the ecoregion in the coming years and how the predicted changes are likely to affect the various conservation elements of interest.

## 5.1 Projected Near-term Future (2025) Development

Several management questions (MQ C2, D6, G1, and G2) required an assessment of the future effects of change agents, especially development, on conservation elements. The year 2025 was selected for this analysis. Projected near-term (2025) development was built from the current development fuzzy logic model, which is comprised of four major development components—energy development, agricultural development, urban and road development, and recreational development (Figure 5-1). In reality, all of these factors are likely to change, but there was a lack of predictive data available to use that provided meaningful projections into the future. Although there were no data for near-term expansion of linear utilities, data did exist for projected near-term oil and gas development (Copeland et al. 2009). The only data provided for projected renewable energy development was a small area of potential wind development in the southwest corner slightly outside the ecoregion boundary. There were no datasets for projected future for either intensive agriculture or grazing. Given climate change results, will agriculture begin to decline in the region? If so, then where? Current recreation data was difficult to acquire and assemble so any future projections based on it would likely be poor as well; as a result, there was no change made in recreation for the near-term. Lastly, future projections for urban development were based on model results from Theobald (2010), but there were no accompanying data on projected road building, which is a noteworthy deficiency as road development precedes urbanization and road impacts on intactness and many wildlife species are well-known. Even with the lack of important topical data, some measurable changes were observed (Table 5-1). The Very High development class increased by 2% and both High and Moderately High classes gained approximately .5%; in all, the development footprint increased by about 1.5 million acres. All of the results from the development model were incorporated into the near-term intactness models except the projected oil and gas development footprint, because the near-term intactness models had already been completed when a new oil and gas dataset arrived in January of 2012 (Copeland et al. 2009). However, the projected oil and gas development footprint was applied to sage grouse because of its importance to that species' future (see sage grouse insert). The potential impact on conservation elements from near-term future development was examined by applying the near-term intactness modeling described in Section 5.3.

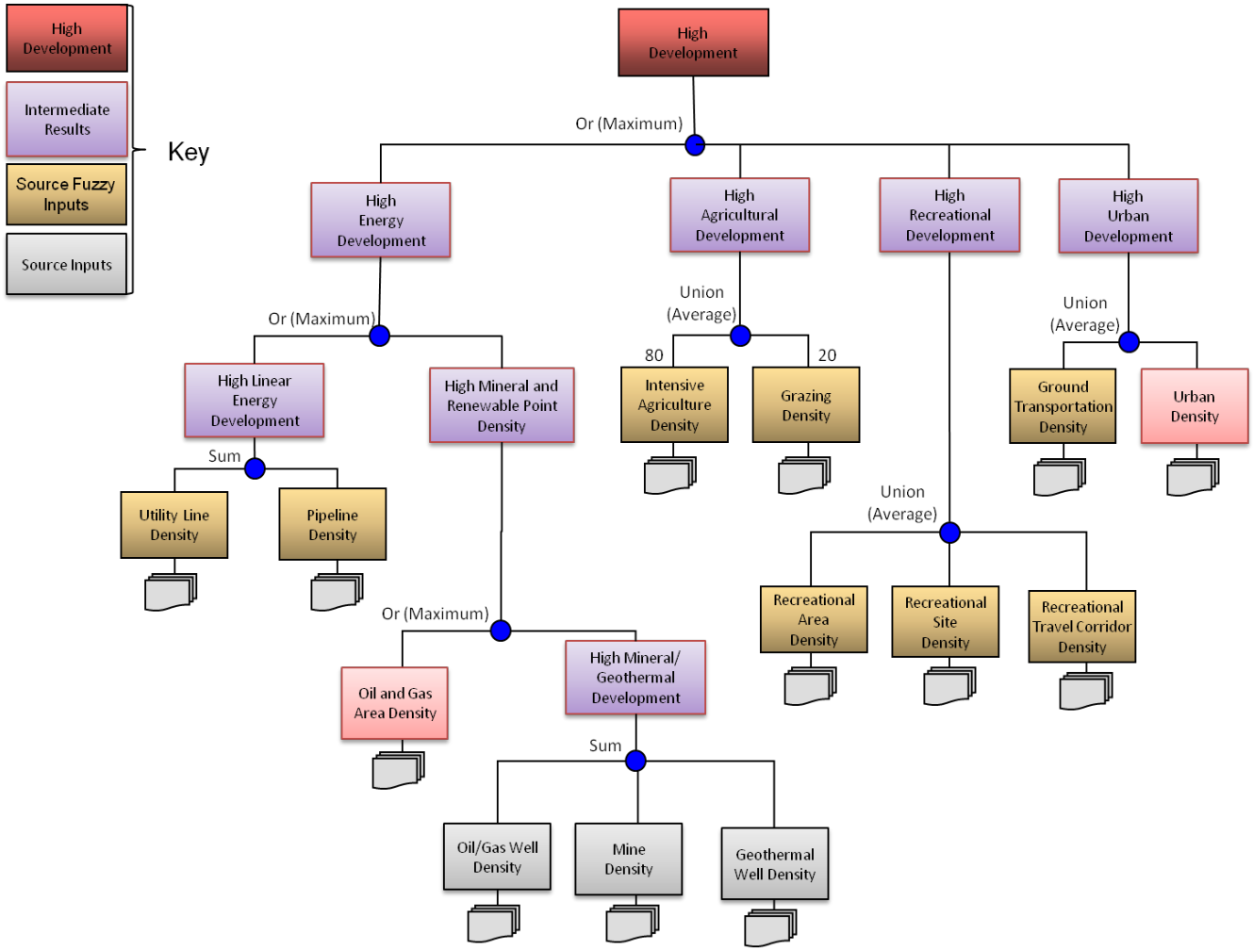


Figure 5-1. Fuzzy logic model for future near-term (2025) development for the Colorado Plateau ecoregion. Projection data existed only for projected near-term oil and gas development and urban expansion (Theobald 2010, pink boxes).

Table 5-1. Modeled change in land area (in 1000s of acres) from increased development 2011–2025. The Very High development class increased by 2% and both High and Moderately High classes gained approximately .5%; in all, the development footprint increased by about 1.5 million acres.

| Category | Current | Percent | Near-term | Percent | Change |
|---|---|---|---|---|---|
| Very High | 4,779 | 10.7% | 5,698 | 12.7% | +2.1% |
| High | 2,270 | 5.1% | 2,553 | 5.7% | +0.6% |
| Moderately High | 4,740 | 10.6% | 5,004 | 11.2% | +0.6% |
| Moderately Low | 13,200 | 29.5% | 12,313 | 27.5% | -2.0% |
| Low | 16,706 | 37.3% | 16,184 | 36.1% | -1.2% |
| Very Low | 3,109 | 6.9% | 3,052 | 6.8% | -0.1% |

## 5.2 Potential Energy Development

Maximum potential (long-term) energy development was also handled with a fuzzy logic model that included three major components—traditional oil and gas, wind energy, and solar energy (Figure 5-2). Potential oil and gas development data included numerous sources—Intermountain West oil and gas potential (Copeland et al. 2009), BLM oil and gas leases, allowable leasing footprints for oil shale and tar sand extraction (2008 data from BLM Oil Shale and Tar Sands Preliminary Environmental Impact Statement), and Department of Energy producing oil and gas fields, mapped by buffering existing active wells by 1.4 km (Figure 5-3). Two data sources comprised potential wind development—Utah BLM wind energy priority Areas and National Renewable Energy Laboratory (NREL) wind power density classes 3 and above at 50 m high (Figure 5-4). Solar resource potential (>5.5 kW/m$^2$) was obtained from NREL as well (Figure 5-5).

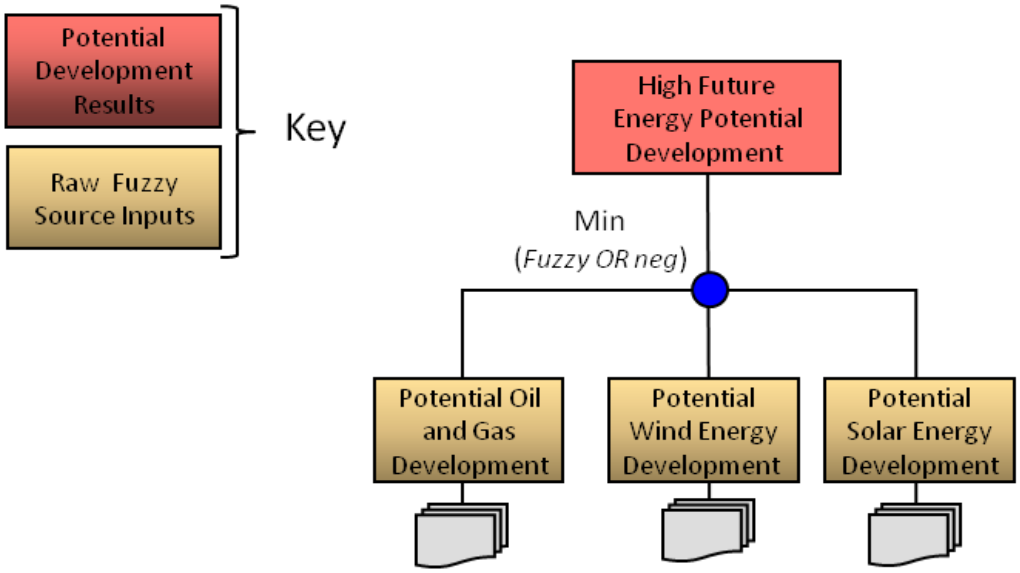


Figure 5-2. Fuzzy logic model diagram for potential energy development in the Colorado Plateau ecoregion.

Summarized at 4km resolution, the final composite map for all three energy components covered a large area of the ecoregion, particularly in the northern and eastern portions (Figure 5-6). Values from the fuzzy logic model were divided into three basic classes (High: 1 to 0.33, Moderate: 0.33 to -0.33, and Low: -0.33 to -1) instead of the six classes that have been used in other fuzzy logic models (such as the intactness models and the model for near-term [2025] development); finer differentiation was not depicted or warranted because the subject data covered broad areas and were more speculative (that is, not based on actual plans for development). For the ecoregion, about 12,500,000 acres (28%) were classified as having High potential, about 5,000,000 acres (12%) Moderate potential, and the rest, over 27,000,000 acres (60%) Low potential. These results were overlaid with the distribution maps for all of the conservation elements to evaluate the potential impact. Designated lands were not included in this part of the analysis because most energy development is prohibited from these areas.

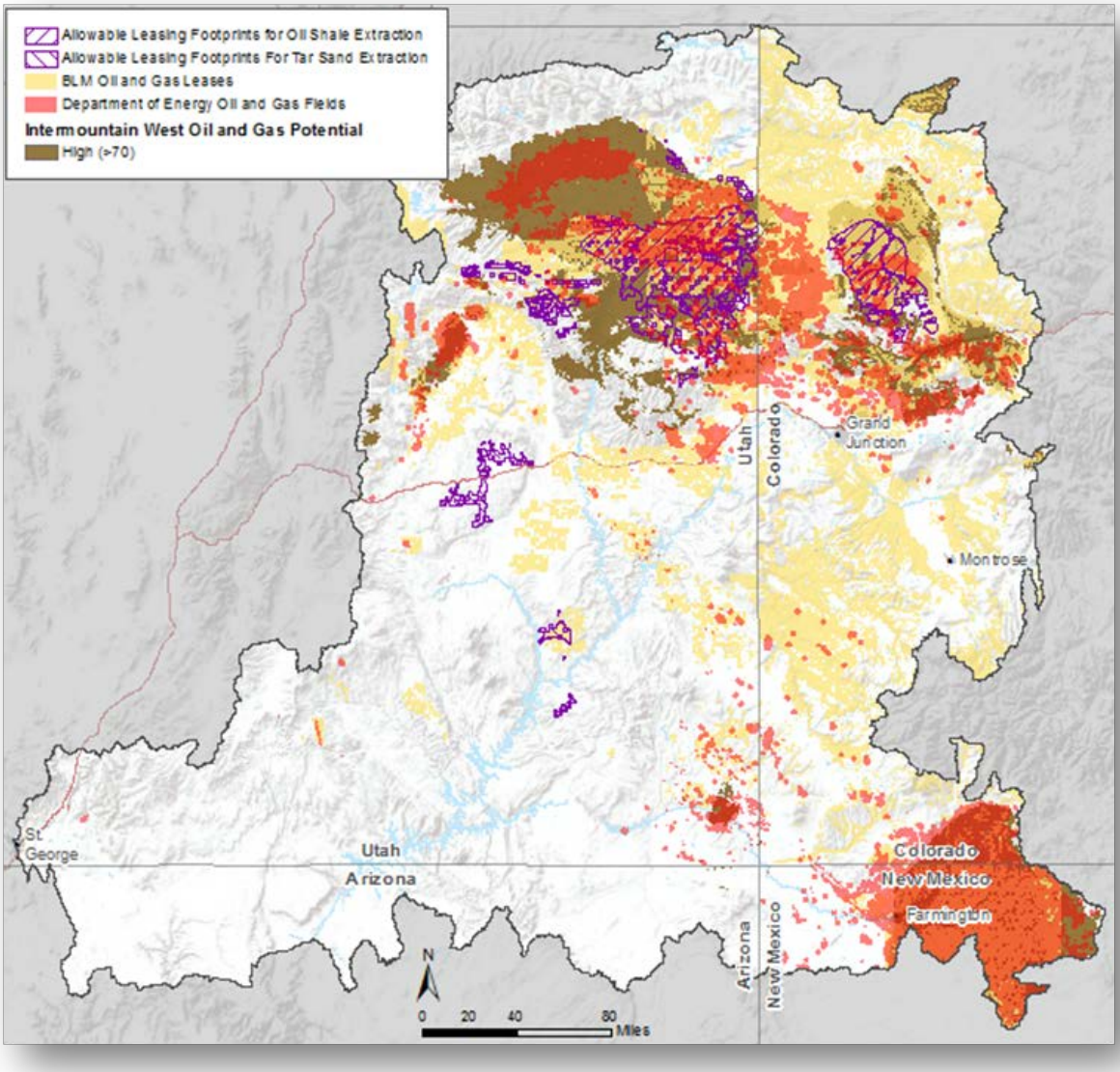


Figure 5-3. Map showing data sources for potential oil and gas development including Intermountain West oil and gas potential (Copeland et al. 2009, brown areas), BLM oil and gas leases (yellow), allowable leasing footprints for oil shale and tar sand extraction (2008 data from BLM Oil Shale and Tar Sands Preliminary Environmental Impact Statement, purple hatched areas), and Department of Energy producing oil and gas fields (orange areas), mapped by buffering existing active wells by 1.4 km.

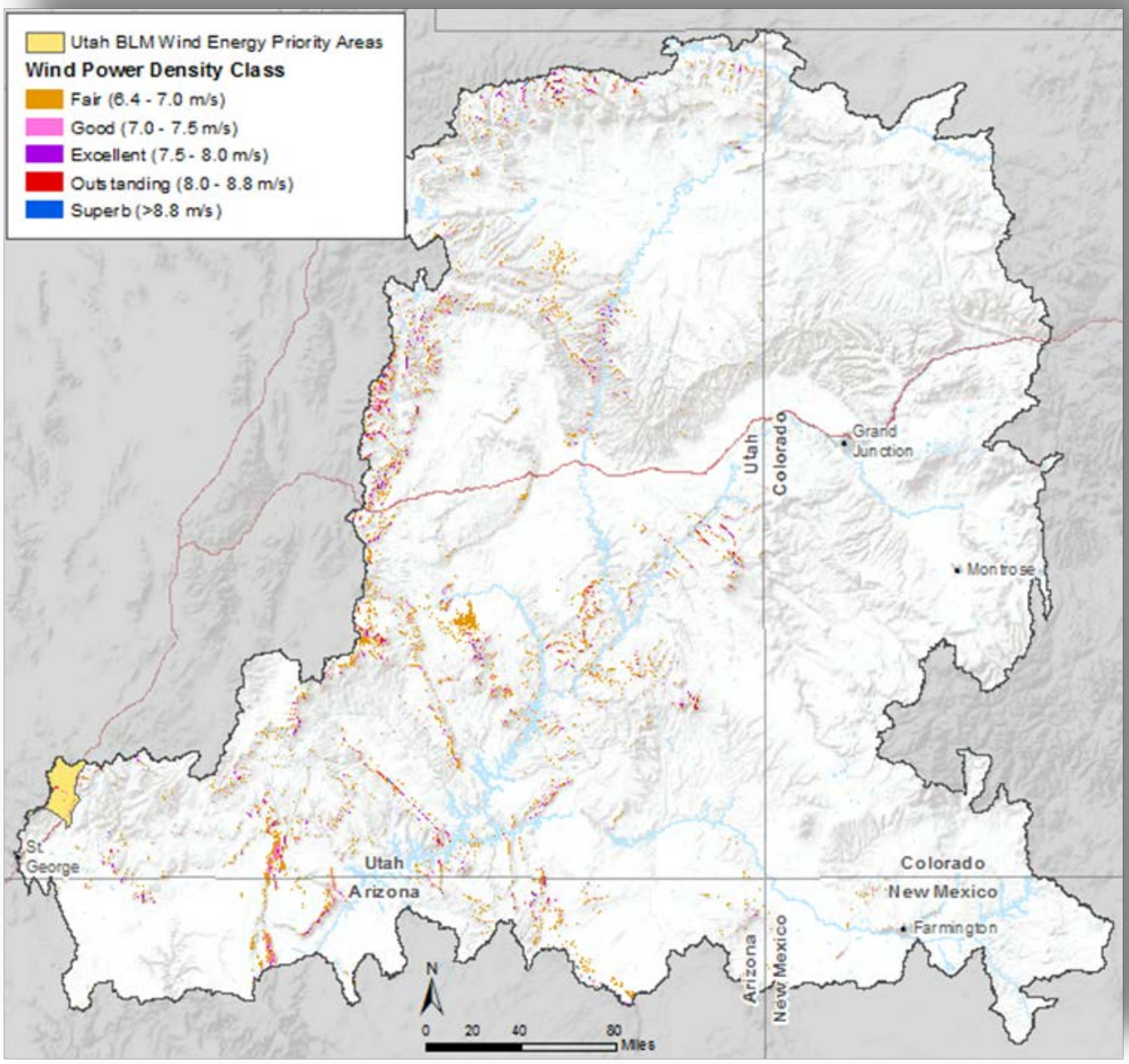


Figure 5-4. Map showing data sources for potential wind development comprised of Utah BLM wind energy priority Areas and National Renewable Energy Laboratory (NREL) wind power density classes 3 and above at 50 m high.

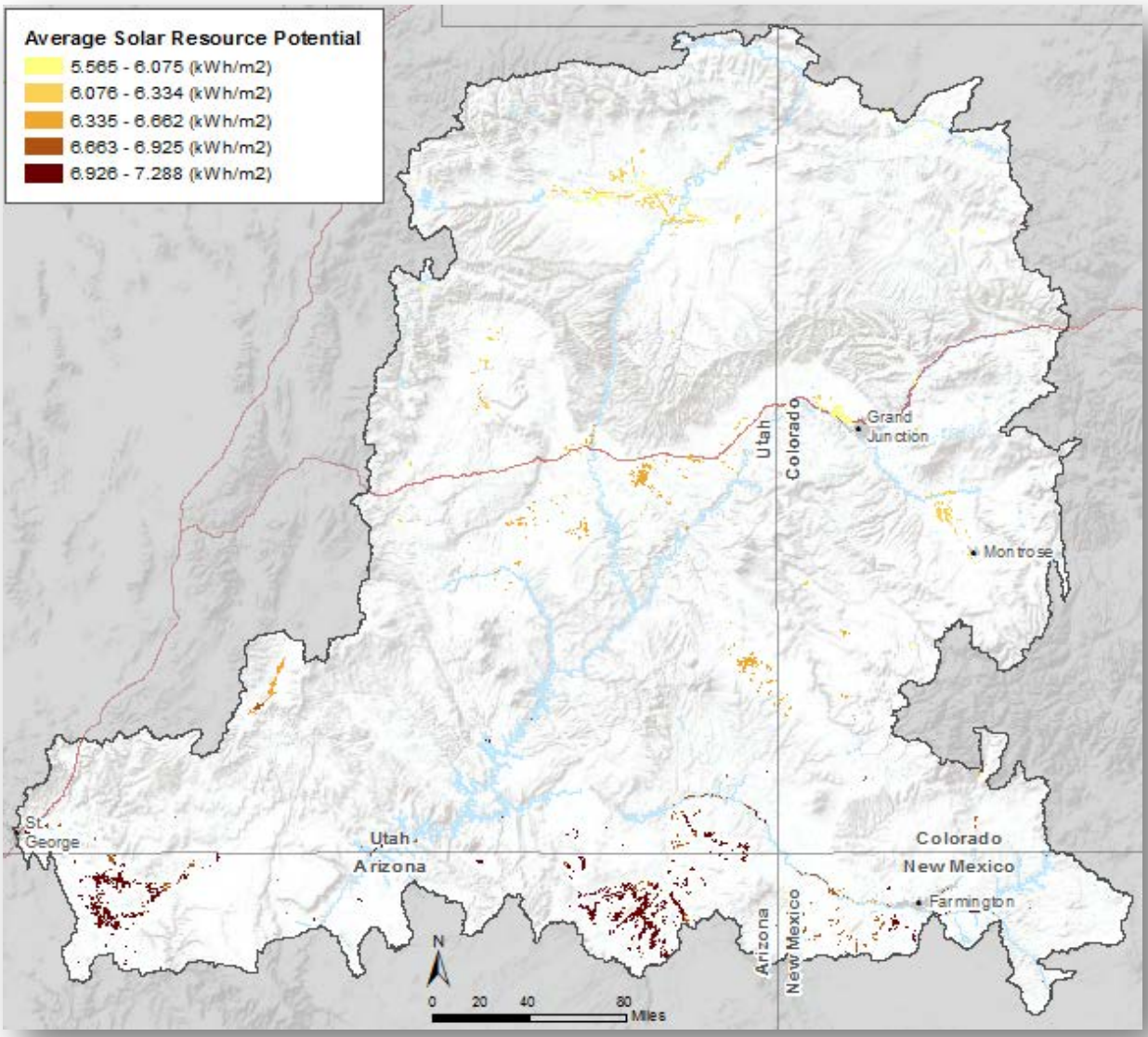


Figure 5-5. Map of solar resource potential (>5.5 kW/m$^2$) obtained from the National Renewable Energy Laboratory (NREL). The highest solar resource potential is in the southern portion of the ecoregion.

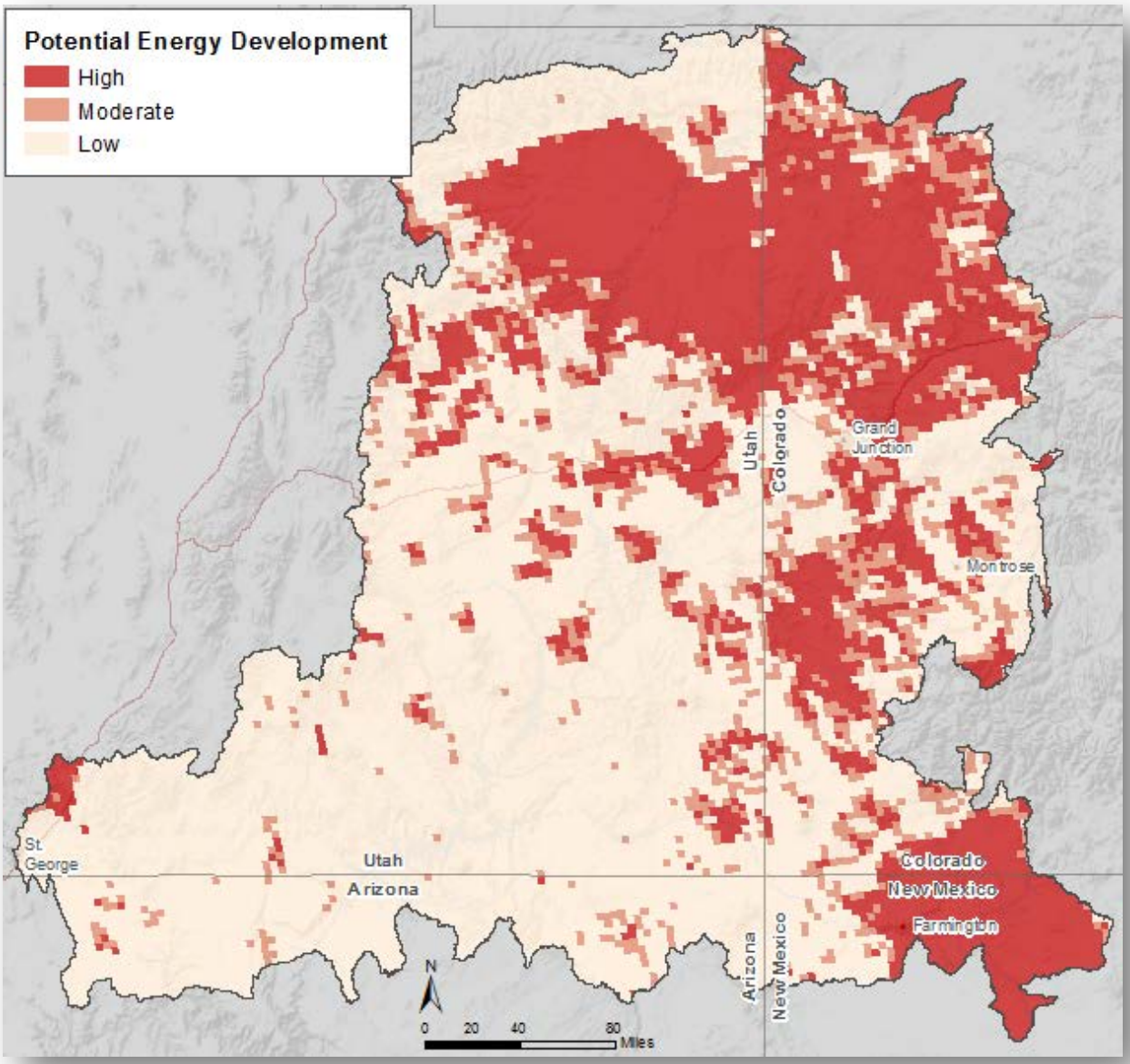


Figure 5-6. Map of potential energy development for all three energy components (oil and gas, wind, and solar energy) in the Colorado Plateau ecoregion. Values from the fuzzy logic model were divided into three basic classes (High 1 to 0.33, Moderate 0.33 to -0.33, and Low -0.33 to -1).

## 5.2.1 Impact of Potential Energy Development on Wildlife Species

Potential impact on species conservation elements from potential (or long term) energy development varied greatly. Of the seven mammal species examined (Figure 5-7), all of the animals with habitat concentrated in the northern portions of the ecoregion showed large potential impacts. Nearly 90% of the extremely limited current black-footed ferret distribution fell within the High risk class. The white-tailed prairie dog, the main prey item for ferrets, had 60% of its current distribution within the High risk class. Pronghorn antelope showed nearly 50% of its current distribution in the High risk class. All of the other species had approximately 30% of their habitat within the High risk category.

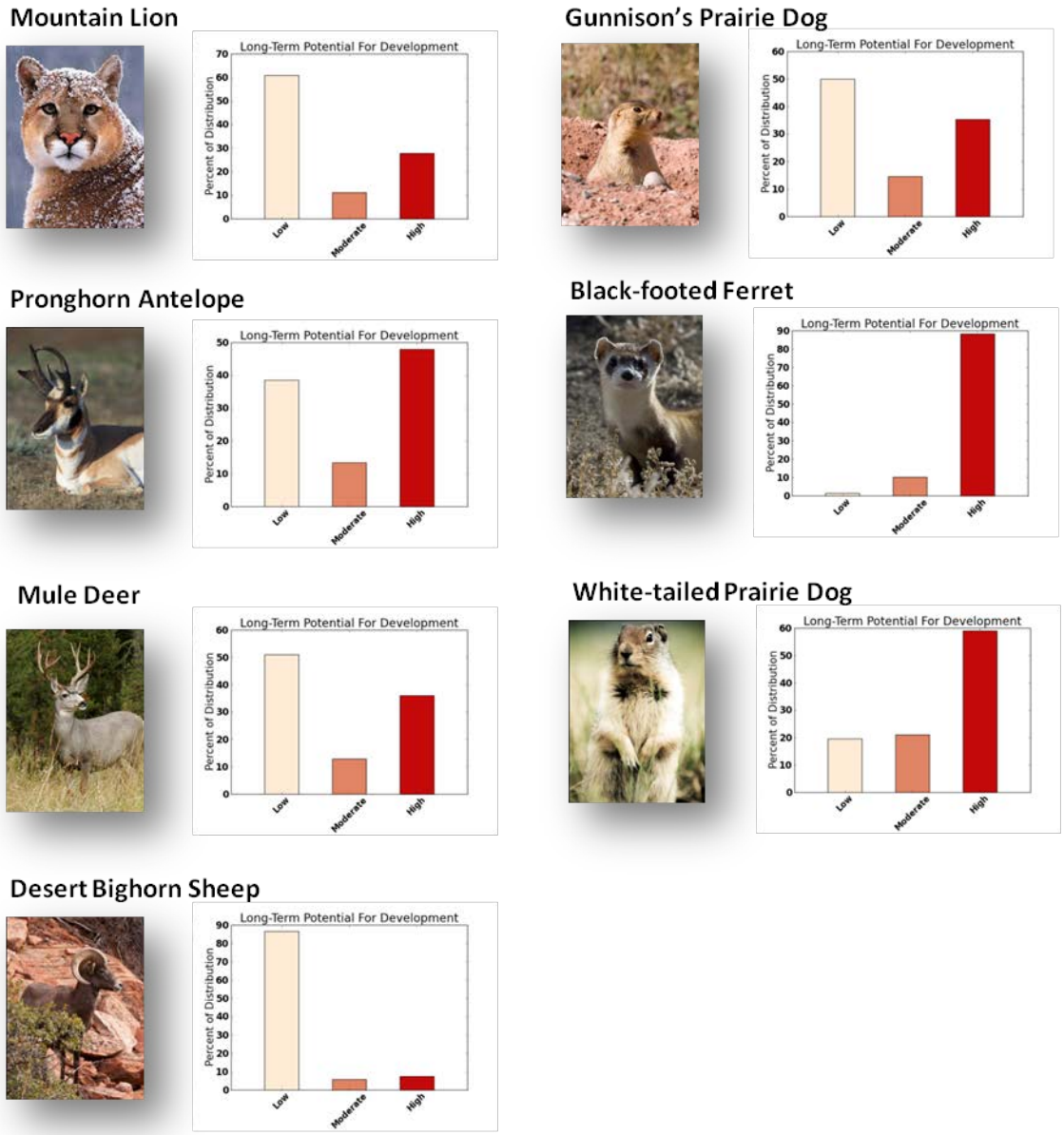


Figure 5-7. Potential impact from energy development for the mammal conservation elements of the Colorado Plateau ecoregion.

Birds showed a variable pattern as well (Figure 5-8). Not surprisingly, greater sage grouse showed the highest risk from potential energy development with nearly 50% of its existing distribution in the High category with another 15% in the Moderate category. Yellow-breasted chat showed high risk as well with 40% High and 18% Moderate, respectively. All of the birds of prey showed similar results with around 30% of their distributions in the High potential class except Mexican spotted owl, which had very little overlap in distribution with energy development. Although Gunnison sage-grouse appears to be less threatened by energy development than greater sage-grouse with about 40% in High and Moderate risk categories, just 1/4 of its distribution (about 100,000 acres) occurs on BLM land subject to energy development. The species has a much more limited distribution than greater sage-grouse, and it is subject to other impacts (rowcrop agriculture, grazing, and some urbanization) on the 2/3 of its distribution that is on private land.

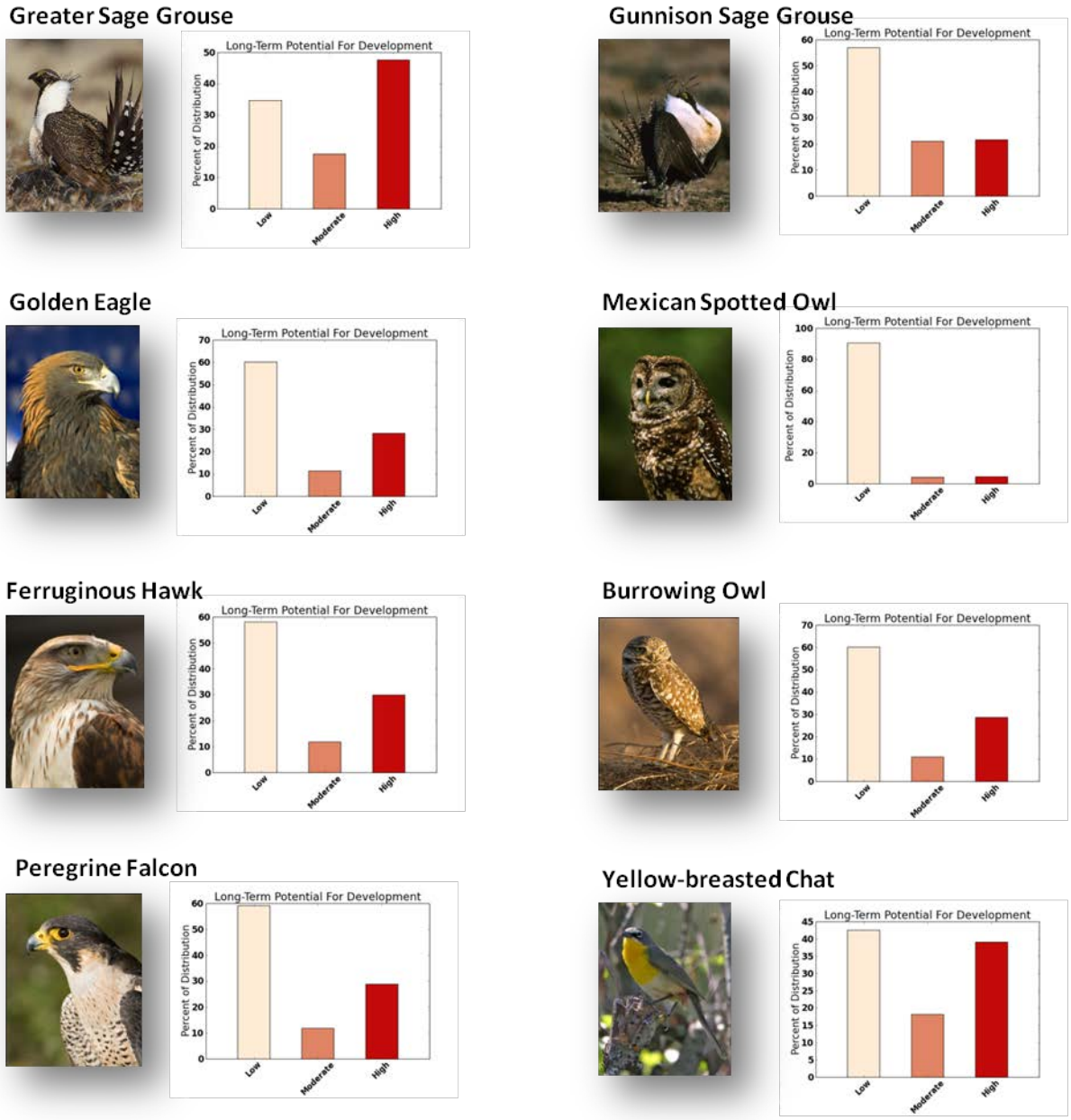


Figure 5-8. Potential impact from energy development for the birds of the Colorado Plateau ecoregion.

## 5.2.2 Potential Energy Development Impact on Vegetation Communities

Of the nine vegetation communities examined, intermountain basins big sagebrush shrubland and pinyon-juniper woodland showed the highest potential for change. Inter-mountain Basins Big Sagebrush Shrubland and Colorado Plateau Pinyon-Juniper Woodland showed over 40% of their current distributions within the High risk class (Figure 5-9). Colorado Plateau Blackbrush-Mormon-tea Shrubland and Mixed Bedrock Canyon and Tableland were least affected by energy development. All other communities had 20-30% of their current distributions at High risk.

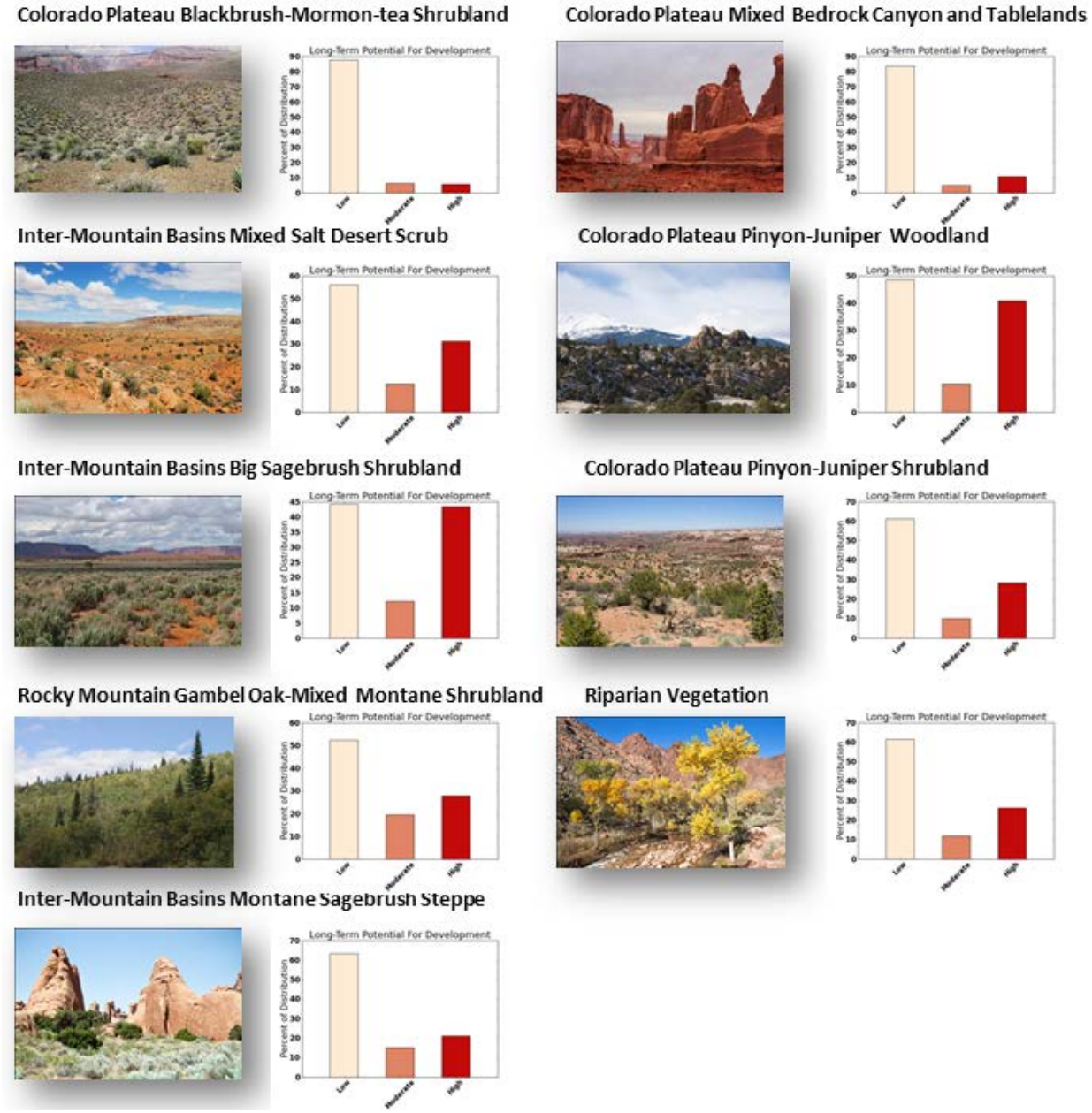


Figure 5-9. Potential impact from energy development for the vegetation communities of the Colorado Plateau ecoregion.

## 5.3 Near-term Future (2025) Terrestrial Landscape Intactness

Near-term (2025) terrestrial landscape intactness models (at both 4km and HUC5 reporting units) consisted of the same components and construction as the current intactness models with available projection datasets used in place of current condition (Figure 5-10). Urban area and invasive projections (pink boxes in logic model) were updated for the terrestrial landscape intactness model. Invasives species projection data was added to current invasive data (LANDFIRE and NatureServe invasives classes, a predictive model of tamarisk distribution [Jarnevich et al. 2011], and historic tamarisk polyline data). Projections of invasive spread were based on LANDFIRE succession class data, which included all invasive species, and US Geological Survey data on early seasonal invasives (Figure 5-11, J. Hansen, T. Arundel, and R. Kokaly, model created in 2011 for this REA). Process models and source maps may be viewed in Appendix A. FRAGSTATS was not rerun because of the coarse resolution of some of the updated invasives data which would have added additional uncertainty to the results. Overall, conditions in the ecoregion showed a decline with modest decreases in Very High and High intactness area countered by slight increases in the other four categories (Figure 5-12). After completing the intactness model for the near-term (2025) future, distribution data was evaluated for each of the conservation elements and their change in status predicted from the near-term change agents for which data existed.

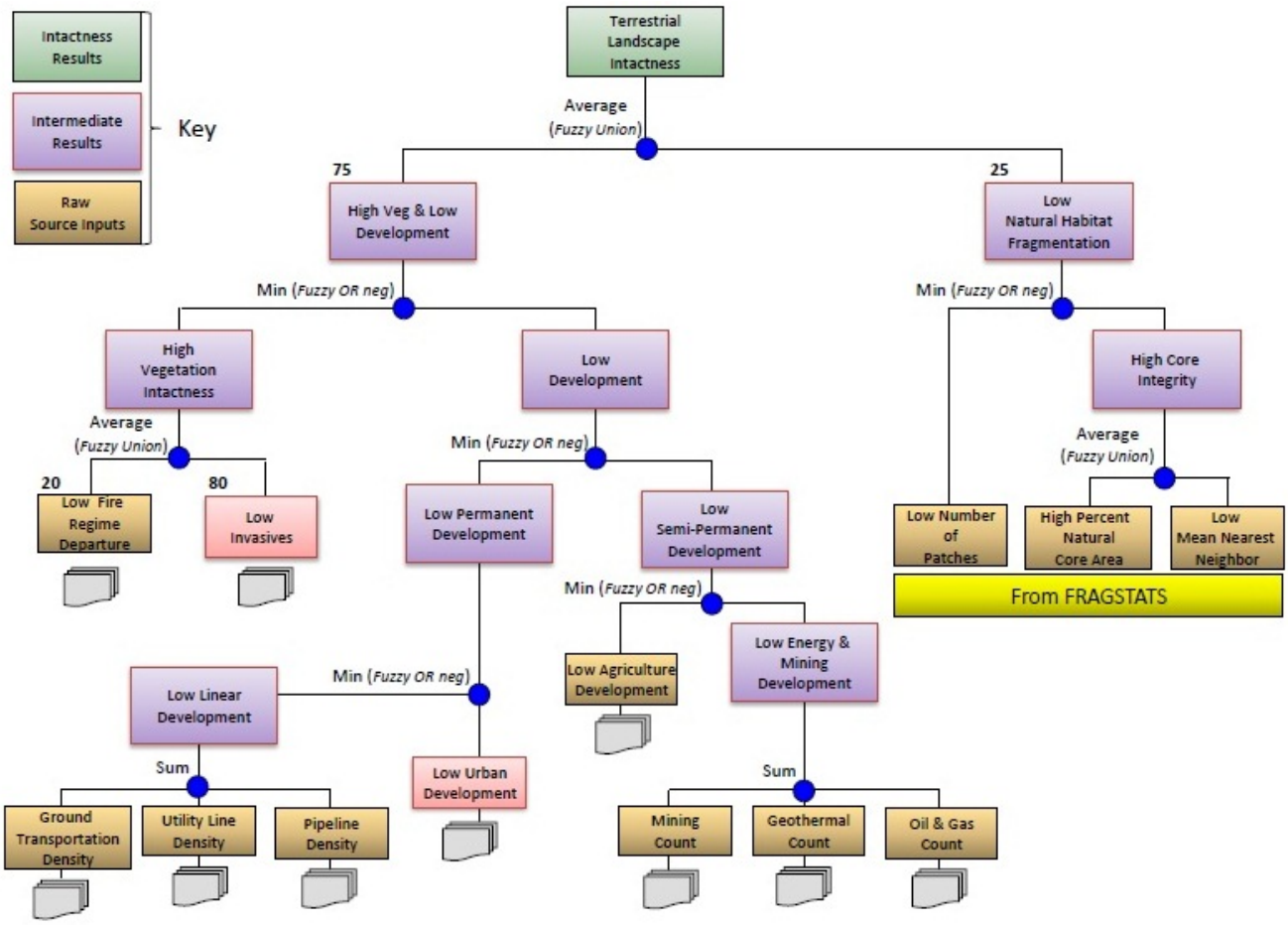


Figure 5-10. Near-term future terrestrial landscape intactness fuzzy logic model.

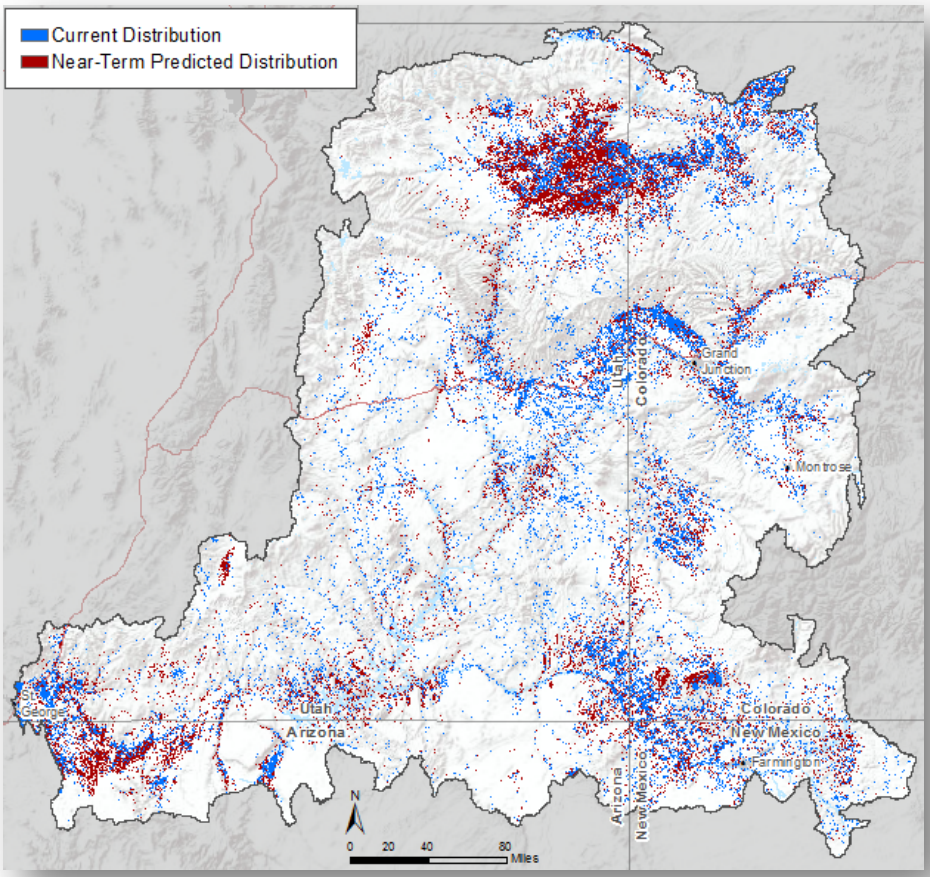


Figure 5-11. Current and near-term future (2025) predicted distribution of invasive species.

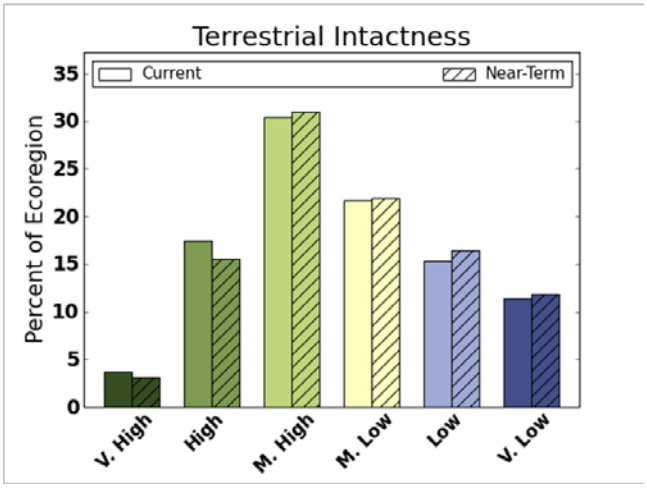


Figure 5-12. Histogram comparing current (solid color bars) and near-term future (hatched bars) terrestrial landscape intactness for the Colorado Plateau showing decreases in Very High and High intactness area and slight increases in the other four categories.

## 5.3.1 Near-Term Future Status for Terrestrial Wildlife Species

Current and near-term status for each conservation element was based on the terrestrial landscape intactness models for the two time periods using the 4km resolution grid. Results pertain to the area of actual occurrence at the finest scale (1:24,000) or resolution (30m pixels) available for that element. Changes are not dramatic; although the model is well-constructed, it is lacking data for some important elements, such as new recreation, roads, agriculture, and grazing. Thus, although changes are small, they are in a negative (lower intactness) direction, as one would expect.

All mammals experienced some declines in status (Figure 5-13), although some species' habitats were in poorer condition based on current conditions. All of the mammal species that inhabit low elevation, open landscapes showed further declines. Black-footed ferret started out with none of its habitat in Very High or High condition and the next class (Moderately High) indicated a drop of approximately two-thirds. Both prairie dog species showed almost all of their remaining High intactness areas eliminated, and pronghorn antelope also had some declines in all three positive classes. Desert bighorn sheep showed the least amount of impact in 2025 even though it too had declines at the highest intactness classes. Mule deer and mountain lion showed similar response to near-term change (Figure 5-13 and Figure 5-14A) when using the same thresholds for the model variables. When the road threshold was applied to the model for mountain lion as described in Chapter 4 (0.60 km/km$^2$, Van Dyke et al. 1986), the declines in mountain lion viability are more dramatic (Figure 14A, histogram on the right). The declines are evident not from the addition of potential roads data (projections on roads were not available) but because road densities representing true (or +1 in fuzzy logic) are constrained in the model to a level that does not negatively affect mountain lion (0.60 km/km$^2$ according to Van Dyke et al. [1986], Figure 5-14A). This is one example of the flexibility of the modeling process that allows quantifiable threshold information to be inserted as it becomes available.

Greater sage-grouse showed the most notable declines in habitat quality of all the bird species, especially when using the oil and gas well density threshold of > 12.3 wells/4 km$^2$ (8 wells/mile$^2$, Figure 5-14B). The most recent Copeland et al. (2009) data on projected oil and gas potential was included for this one species only. The oil and gas projection data [Copeland et al. 2009] was not applied to Gunnison sage-grouse because none of the projections included in the Copeland et al. (2009) study occurred within its distribution.

Gunnison sage-grouse showed minimal change (Figure 5-14C); however, of all the bird species, Gunnison sage-grouse presently inhabits the least intact habitats, comparable in quality to the habitats of black-footed ferret and the two prairie dog species. Two-thirds of the distribution of Gunnison sage-grouse is on private agricultural or grazing lands that are not at high risk of major transformation in the near-term future except for possible oil and gas development on private land for which there was no projection data. The other bird species, all with a wider range of more intact habitat classes in the present time period, showed consistent declines in the higher quality intactness classes with matching increases in the lower classes in the near-term future (Figure 5-15).

## 5.3.2 Near-Term Future Status for Aquatic Wildlife Species

The only change made in the aquatic intactness model was the addition of new urban areas for the 2025 time frame. No other data was available to populate the model whether it was planned dams and diversion changes, road construction, or chemical discharge and pesticide application changes. All of these have tremendous impact on aquatic systems for which there was no mechanism to predict into the future. All three fish species primarily showed areas shifting from Low to Very Low aquatic intactness, which by our definition affects their overall status (Figure 5-16).

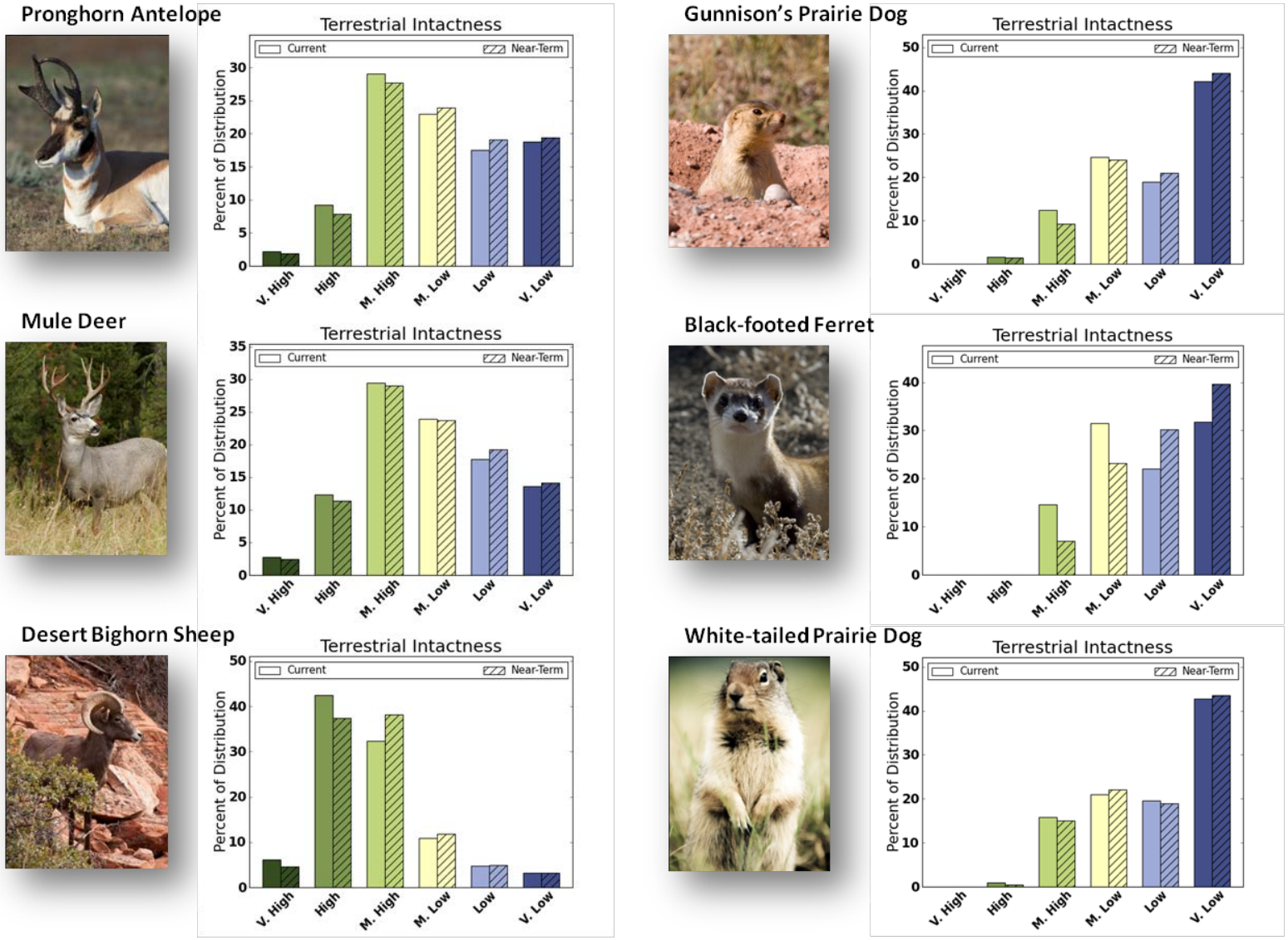


Figure 5-13. Comparison between current (solid) and near-term future (crosshatched) status for mammals.

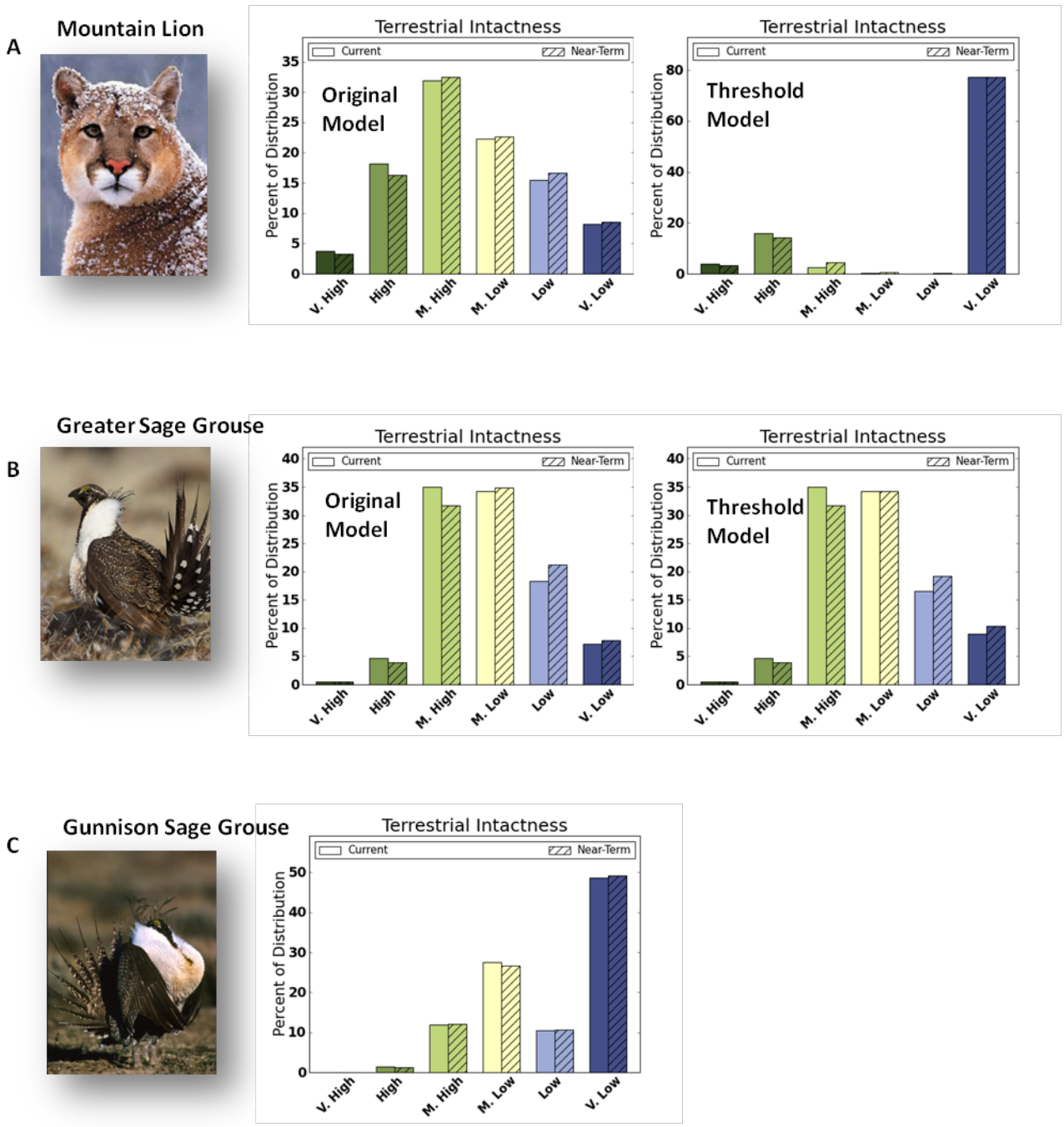


Figure 5-14. A) Comparison of current and near-term future status for mountain lion based on terrestrial landscape intactness for both original and road density threshold (0.60 km/km$^2$, Van Dyke et al. 1986) model versions; (B) greater sage-grouse current and near-term future status based on original model and near-term future version using additional energy projection data (Copeland et al. 2009) and the >12.3 wells/4 km$^2$ (8 wells/mile$^2$) well-density threshold for greater sage-grouse winter habitat (Doherty 2008); and (C) Gunnison sage-grouse current and near-term future status based on original intactness model. (No recently acquired oil and gas data [Copeland et al. 2009] occurred within the distribution of this species.)

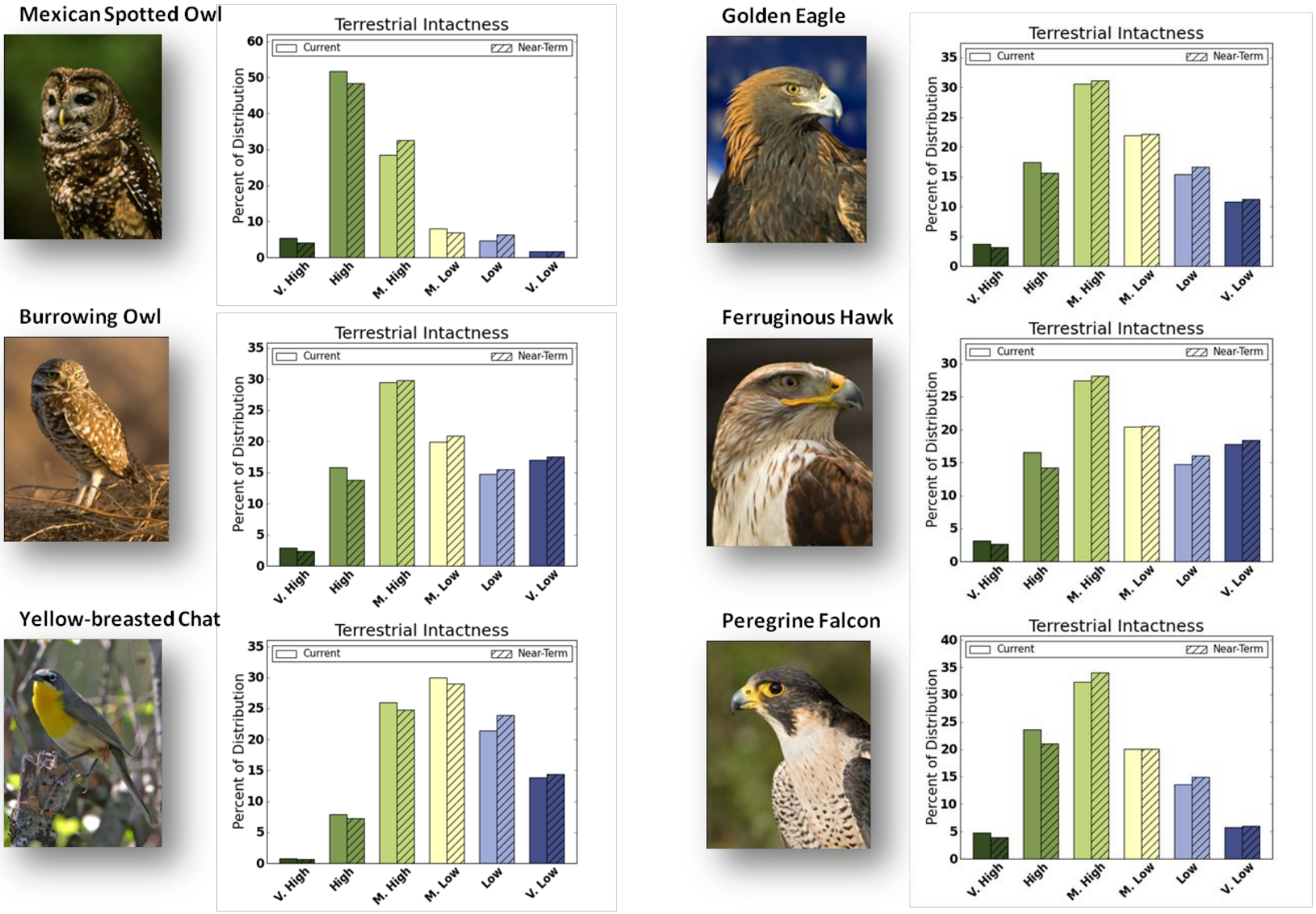


Figure 5-15. Comparison between current (solid bars) and near-term future (2025, crosshatched bars) status for birds.

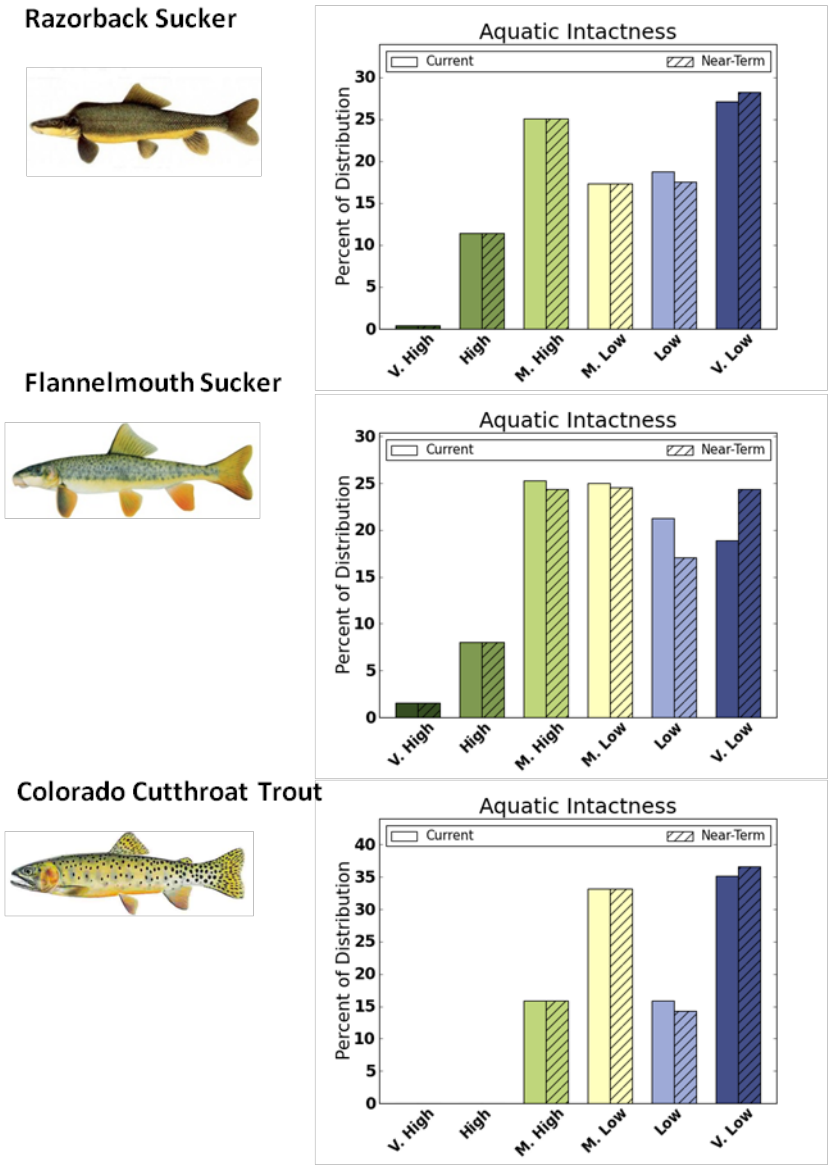


Figure 5-16. Comparison between current (solid bars) and near-term (crosshatched bars) status for fishes based on aquatic intactness.

## 5.3.3 Near-term Future Status for Designated Lands

Changes in near-term future intactness showed small percentage changes in the status of the existing designated lands in the Colorado Plateau ecoregion (Figure 5-17). Most of this is due to the projected increase in invasive species although some designated lands are already located near developed areas, some of which are expected to expand over time, further degrading lands around these sites. Information on the predicted near-term change in status for the remaining sites conservation elements (e.g., biodiversity sites, herd management areas) can be found in Appendix A.

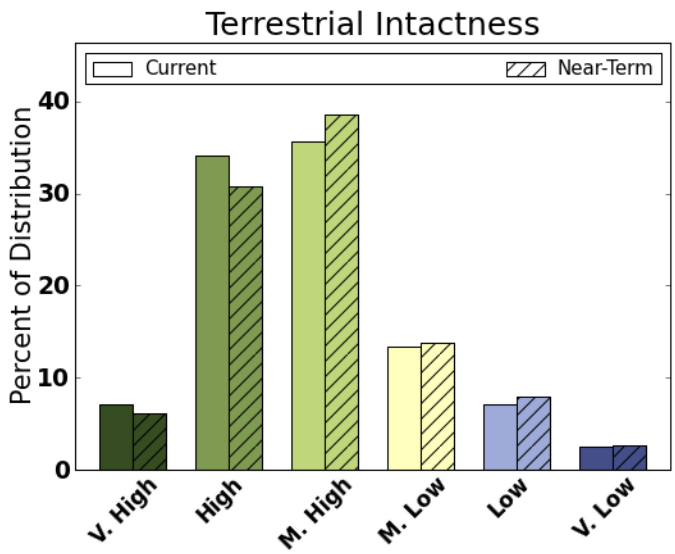


Figure 5-17. Current and near-term (2025) future for status of designated lands in the Colorado plateau ecoregion.

## 5.3.4 Near-term Future Status for Vegetation Communities

Changes in status from current to near-term future for vegetation communities are presented in Figure 5-18 through Figure 5-20. Near-term terrestrial intactness results showed habitat quality declines in all vegetation communities with the greatest declines observed for the two dominant communities—Colorado Plateau Pinyon-Juniper Woodland and Inter-Mountain Basins Big sagebrush Shrubland (Figure 5-18 and 5-19). The least change was observed in the more sparsely vegetated community types such as Colorado Plateau Mixed Bedrock Canyon and Tablelands (Figure 5-18) and Colorado Plateau Blackbrush-Mormon-tea Shrubland (Figure 5-20).

**Colorado Plateau Mixed Bedrock Canyon and Tablelands**

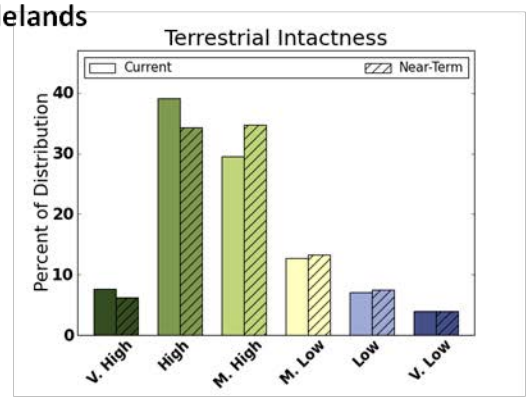


**Colorado Plateau Pinyon-Juniper Woodland**

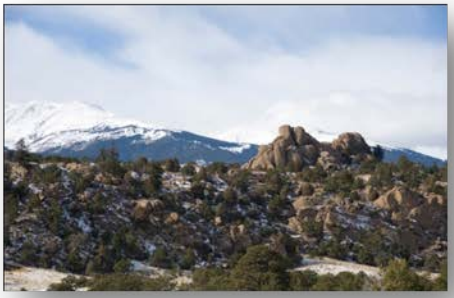

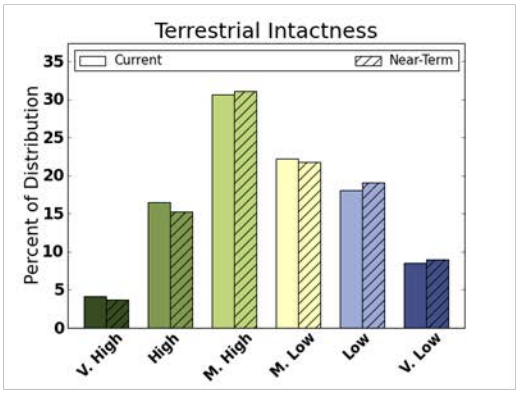


**Colorado Plateau Pinyon-Juniper Shrubland**

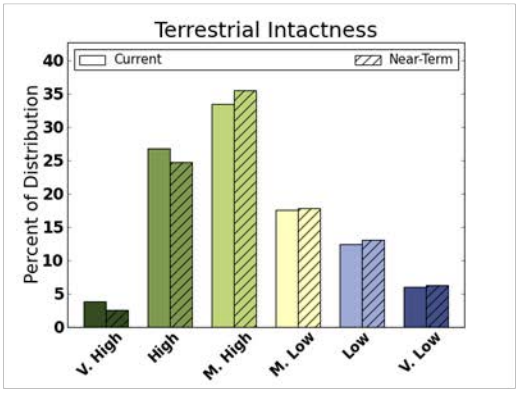


Figure 5-18. Comparison between current (solid) and near-term (crosshatched) status for Colorado Plateau Mixed Bedrock Canyon and Tablelands, Colorado Plateau Pinyon-Juniper Woodland, and Colorado Plateau Pinyon-Juniper Shrubland according to NatureServe Landcover v 2.7 for the Colorado Plateau ecoregion.

**Inter-Mountain Basins Big Sagebrush Shrubland**

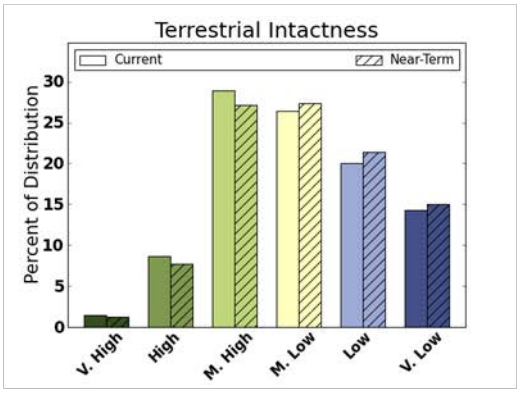


**Inter-Mountain Basins Montane Sagebrush Steppe**

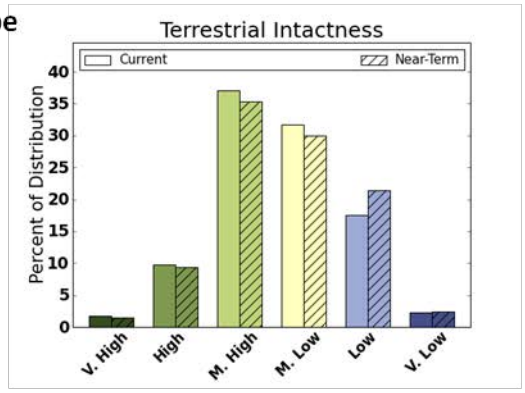


**Riparian Vegetation**

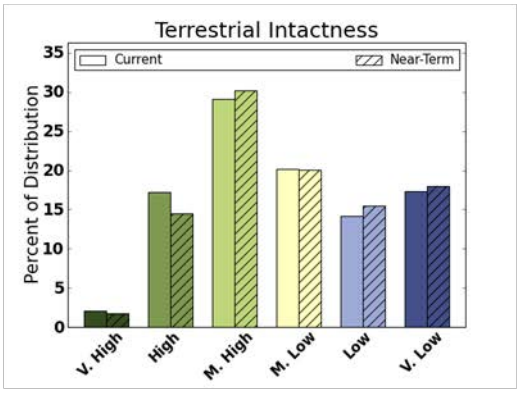


Figure 5-19. Comparison between current (solid) and near-term (crosshatched) status for Inter-Mountains Basins Big Sagebrush Shrubland, Inter-Mountain Basins Montane Sagebrush Steppe, and Riparian vegetation according to NatureServe Landcover v 2.7 for the Colorado Plateau ecoregion.

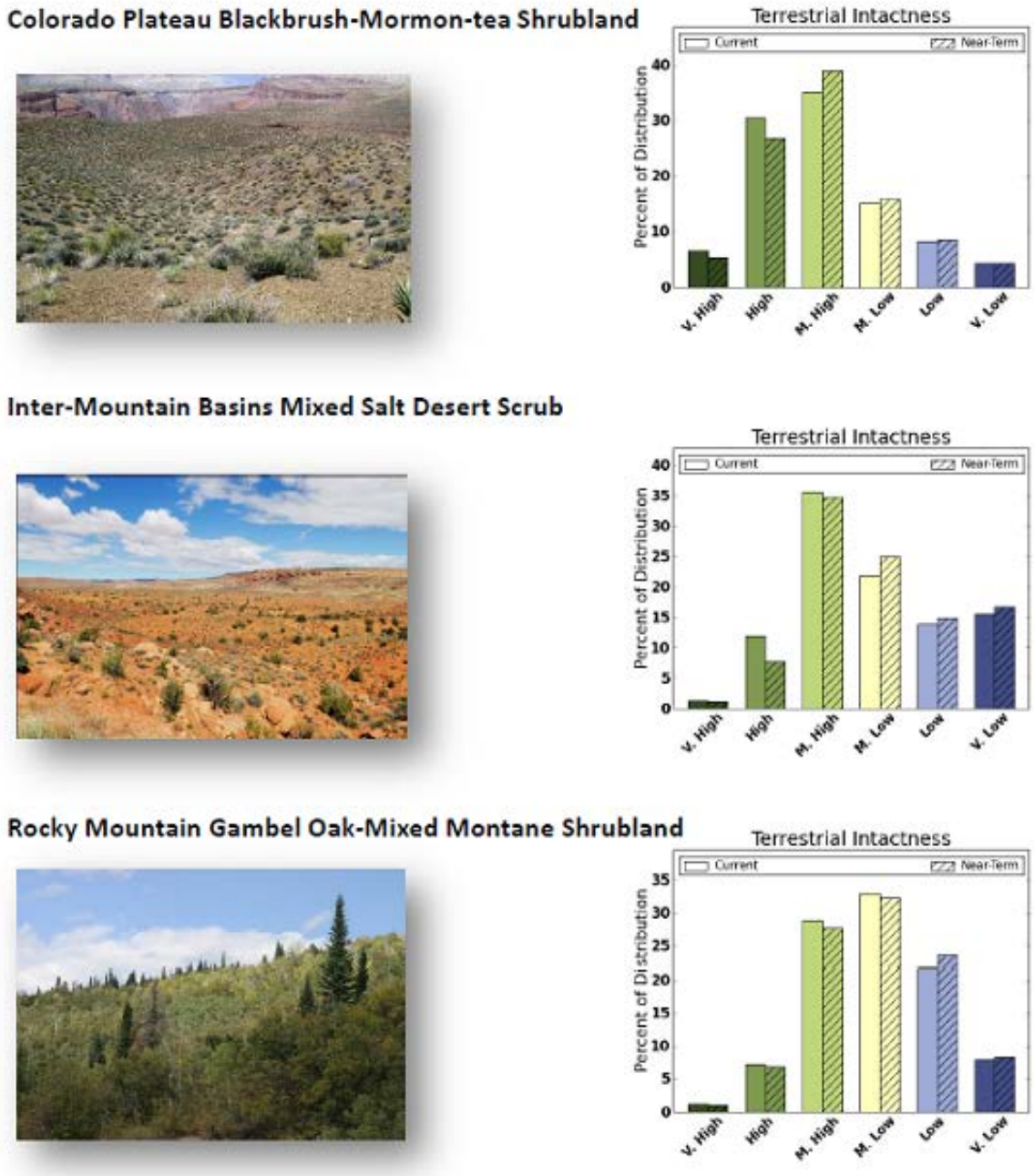


Figure 5-20. Comparison between current (solid) and near-term (crosshatched) status for Colorado Plateau Blackbrush-Mormon-tea Shrubland, Inter-Mountains Basins Mixed Salt Desert Scrub, and Rocky Mountain Gambel Oak-Mixed Montane Shrubland according to NatureServe Landcover v 2.7 for the Colorado Plateau ecoregion.

## 5.4 Climate Change

Climate change results for the Colorado Plateau ecoregion are extensive and complex. Although three different future climate projections were investigated, the ECHAM5-driven RegCM3 climate projections were selected for the body of the report to evaluate potential impact on the various conservation elements. ECHAM5 is the fifth generation of the ECHAM global general circulation model (GCM) developed at the Max Planck Institute in Hamburg, Germany; it has been identified as one of the better models to represent natural climate variability (Mote et al. 2010, Garfin et al. 2010). The other two projections, the GFDL- and GENMOM-driven RegCM3, had results that were wetter overall than many of the other published climate projections (IPCC 2007). The regional RegCM3 model had been chosen because of its representation of the North American Monsoon (Hostetler et al. 2011) which is important to Colorado Plateau vegetation dynamics.

### 5.4.1 Climate Projections

As explained in detail in Chapter 3, Methodology, the climate model data provided by Hostetler et al. (2011) were assembled for two time periods (2015–2030 and 2045–2060), and data from the 2045–2060 time period were used to evaluate the conservation elements, which are presented later in this section. For both temperature and precipitation results, water bodies were left as holes in the modeled data because they create their own local climate conditions and are thus areas of greater uncertainty for the climate model to simulate. Weather stations are rarely placed near water bodies because they would be skewed towards these very local conditions and would not represent broad patterns over the landscape.

Differences in temperature projections—average annual temperature (Figure 5-21), seasonal summer temperature (July–September; Figure 5-22), and winter temperature (January–March; Figure 5-23)—were calculated between historical (1968–1999) and future time periods (2015–2030 and 2045–2060) as simulated by the ECHAM5-driven RegCM3 model. The differences were then used to modify the PRISM historic baseline for 1968–1999. Results show that the ecoregion is expected to undergo general warming over the entire region with as much as 2° Celsius increase by 2060 in some locations, particularly in the southern portion of the ecoregion. Average summer temperatures are expected to increase, but even greater increases are simulated for the winter months. Downscaled climate modeling for the southern Colorado Plateau by Garfin et al. (2010) predicted even greater warming of 4.7° Celsius by the end of the century.

It is generally accepted that climate models are less reliable in simulating precipitation than temperature. There was a large bias in the RegCM3 simulations of historical precipitation for this region. Consequently we had to bias-correct the climate model results to provide more realistic climate input to the vegetation model. We generated future climate projections (precipitation maps Figures 5-25 through 5-27, top row maps 2 and 3) by calculating the ratios between future and historical precipitation values simulated by RegCM3 and multiplying them by the historical PRISM baseline. Under RegCM3 projections, precipitation is expected to decline throughout much of the year during the 2015–2030 time period (with the exception of a couple months in the fall) with severe drought likely to occur in some areas (graph in Figure 5-24 and Figure 5-25). The 2045–2060 time period remains drier (or comparable to historic conditions) during most of the year, but sporadic wetter months (e.g., February, June, and October in Figure 5-24) result in some areas expressing overall projected increases in annual precipitation (Figure 5-25). Considerable variability can be seen when the graphed data is expressed spatially in the precipitation map figures (Figures 5-25 to 5-27). For the seasonal results, summer (Jul–Sep, Figure 5-26) showed more spatial variability in precipitation than did the winter season (Jan–Mar, Figure 5-27).

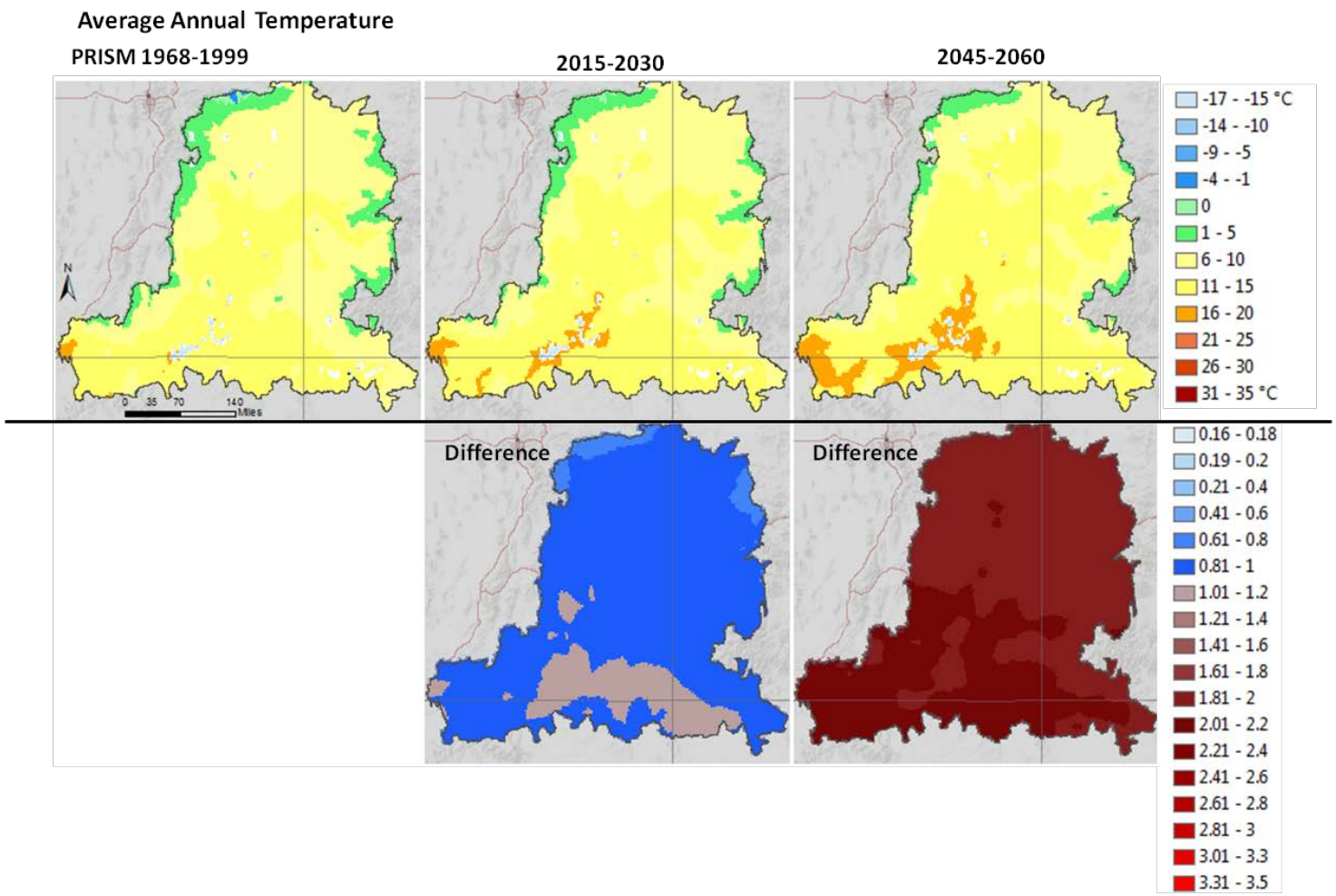


Figure 5-21. Map results for change in raw average annual temperature. Top Row: 1) Observed average annual temperature from PRISM averaged over the historical period (1968–1999 baseline) for the Colorado Plateau ecoregion.; 2-3) Bias-corrected future temperature using the ECHAM5-driven RegCM3 regional climate model deltas modifying the PRISM baseline (1) and averaged for two future time periods. Bottom row: Simulated ECHAM5-driven RegCM3 regional climate model differences between historical (1968–1999) and future (2015–2030; 2045–2060) average annual temperature. All colors on the difference maps are warmer than historic. Note: Bias correction was applied to the climate model results for more realistic climate input to the vegetation model. Future climate projections (top row 2-3) were generated by calculating the differences between future and historical temperature values simulated by RegCM3 (bottom row) and adding them to the historical PRISM baseline (top row).

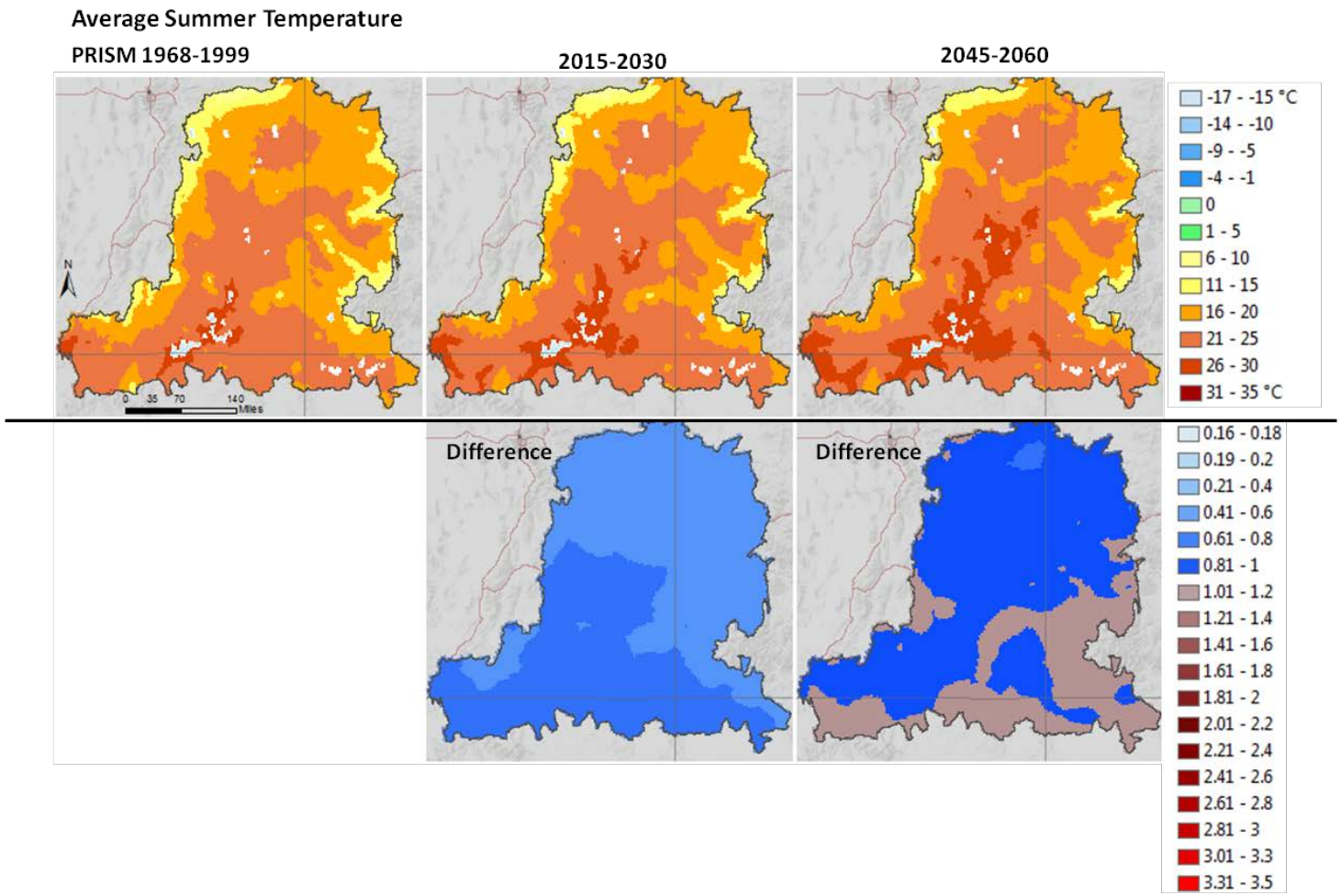


Figure 5-22. Map results for change in raw average summer temperature. Top Row: 1) Observed average summer (July–September) temperature from PRISM averaged over the historical period (1968–1999 baseline) for the Colorado Plateau ecoregion.; 2-3) Bias-corrected future summer temperature using the ECHAM5-driven RegCM3 regional climate model deltas modifying the PRISM baseline (1), and averaged for two future time periods. Bottom row: Simulated ECHAM5-driven RegCM3 regional climate model differences between historical (1968–1999) and future (2015–2030; 2045–2060) average summer temperature. All colors on the difference maps are warmer than historic. Note: Bias correction was applied to the climate model results for more realistic climate input to the vegetation model. Future climate projections (top row 2-3) were generated by calculating the differences between future and historical temperature values simulated by RegCM3 (bottom row) and adding them to the historical PRISM baseline (top row).

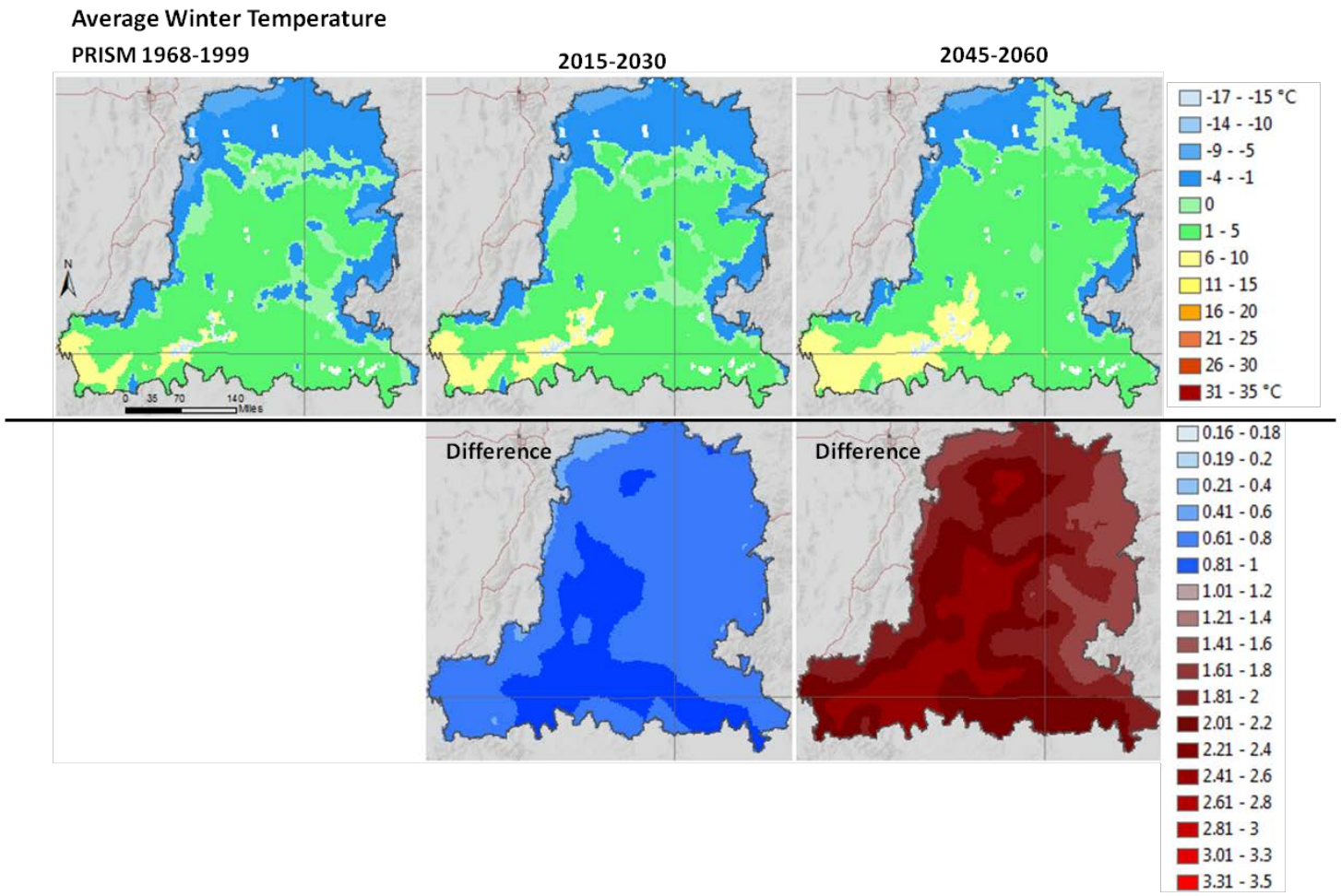


Figure 5-23. Map results for change in raw average winter temperature. Top Row: 1) Observed average winter (January–March) temperature from PRISM averaged over the historical period (1968–1999 baseline) for the Colorado Plateau ecoregion; 2-3) Bias-corrected future winter temperature using the ECHAM5-driven RegCM3 regional climate model deltas modifying the PRISM baseline (1), and averaged for two future time periods. Bottom row: Simulated ECHAM5-driven RegCM3 regional climate model differences between historical (1968–1999) and future (2015–2030; 2045–2060) average winter temperature. All colors on the difference maps are warmer than historic. Note: Bias correction was applied to the climate model results for more realistic climate input to the vegetation model. Future climate projections (top row 2–3) were generated by calculating the differences between future and historical temperature values simulated by RegCM3 (bottom row) and adding them to the historical PRISM baseline (top row).

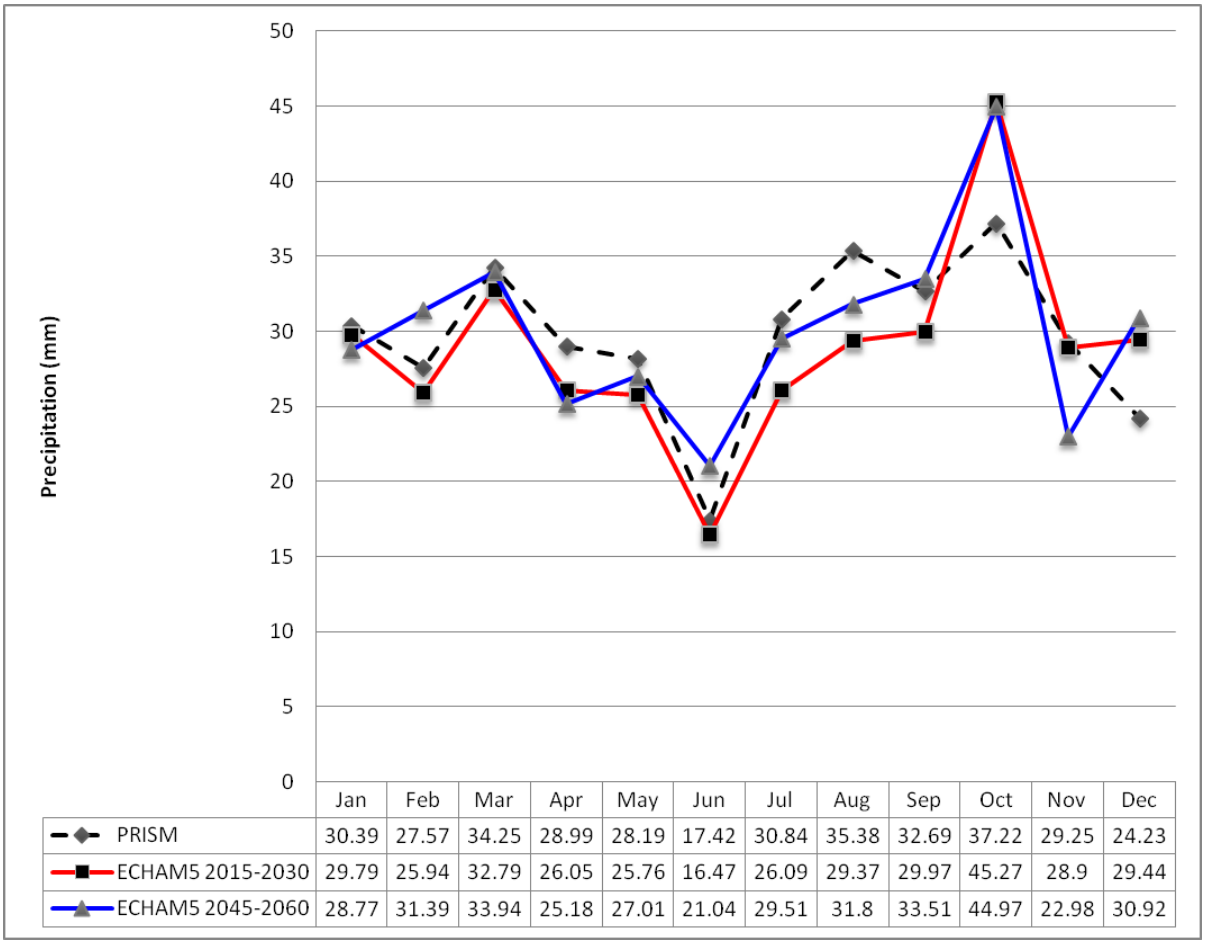


| | Jan | Feb | Mar | Apr | May | Jun | Jul | Aug | Sep | Oct | Nov | Dec |
|---|---|---|---|---|---|---|---|---|---|---|---|---|
| PRISM | 30.39 | 27.57 | 34.25 | 28.99 | 28.19 | 17.42 | 30.84 | 35.38 | 32.69 | 37.22 | 29.25 | 24.23 |
| ECHAM5 2015-2030 | 29.79 | 25.94 | 32.79 | 26.05 | 25.76 | 16.47 | 26.09 | 29.37 | 29.97 | 45.27 | 28.9 | 29.44 |
| ECHAM5 2045-2060 | 28.77 | 31.39 | 33.94 | 25.18 | 27.01 | 21.04 | 29.51 | 31.8 | 33.51 | 44.97 | 22.98 | 30.92 |

Figure 5-24. Graph of average precipitation for each month for each evaluated time period (PRISM=historic 1968–1999) and two future time windows (2015–2030 and 2045–2060) based on the RegCM3 using ECHAM5 boundary conditions.

Using ECHAM-5 GCM projections, Garfin et al (2010) found a 30% decrease in summer precipitation for the southern Colorado Plateau in 2050, as compared to only a 6.5% decline in annual precipitation using an ensemble approach of general circulation model (GCM) projections. Seager et al (2007), using the ensemble mean of 19 GCMs (from the Intergovernmental Panel on Climate Change [IPCC] Fourth Assessment Report [AR4] for the 20th and 21st centuries) and looking at the difference between projected precipitation and evaporation in the Southwest region, warned of future droughts more intense than those recorded during the Dust Bowl of the 1930s and the U.S. droughts of the 1950s.

This (regional) RegCM3 result does not necessarily agree precisely with (global) GCMs. In the past, assessments have used coarse general circulation model projections statistically downscaled to the landscape of interest. Regional climate models are run at finer scales and take into account local processes that are not detected by global climate models. Disagreement or differences in the magnitude of changes between the two types is to be expected. A full interpretation of which is correct is beyond the scope of this assessment but available for debate and comparison to observed records during the historical period.

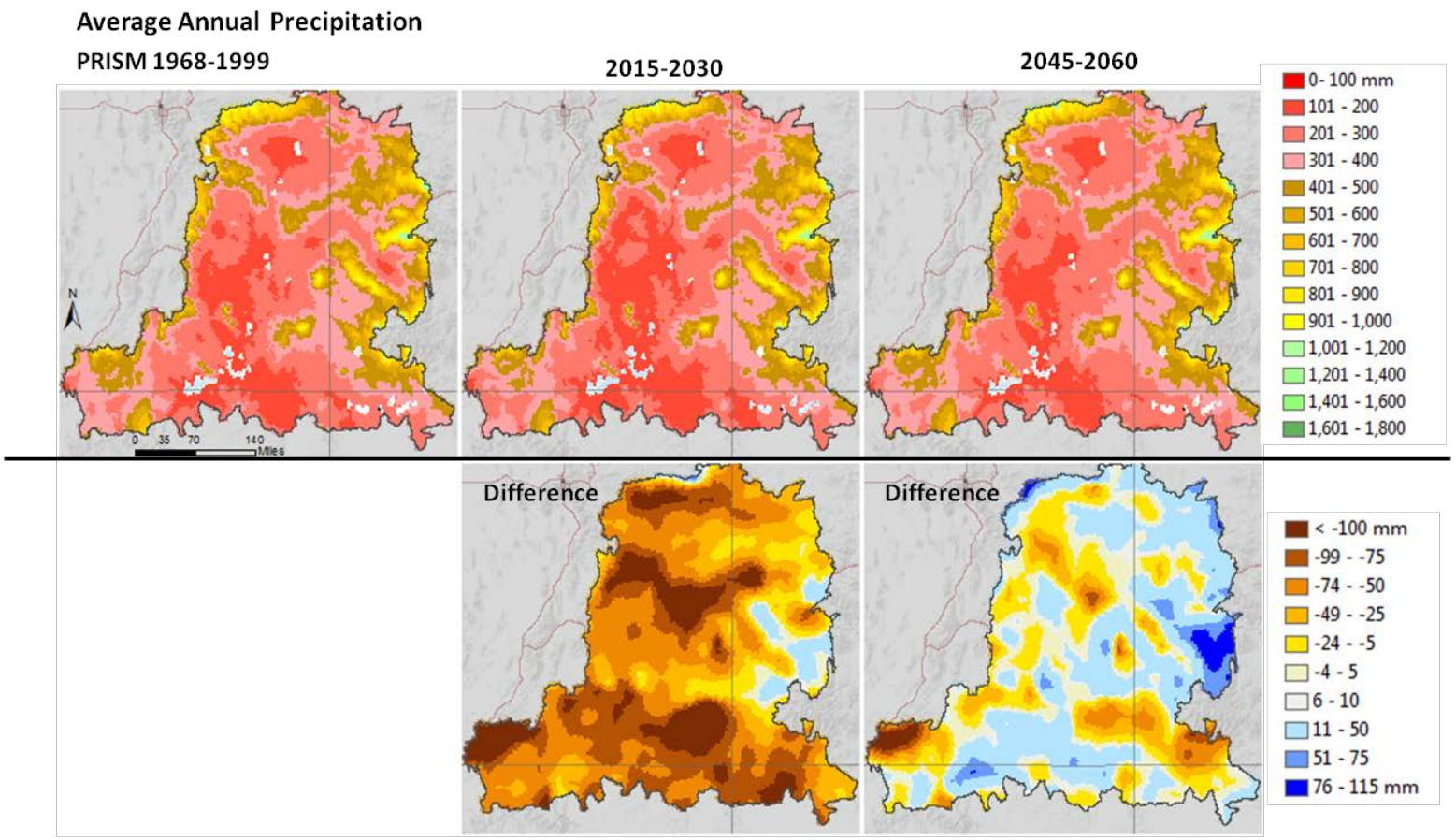


Figure 5-25. Map results for change in average annual precipitation. Top Row: 1) Observed average annual precipitation from PRISM averaged over the historical period (1968–1999 baseline) for the Colorado Plateau ecoregion.; 2-3) Bias-corrected future precipitation using the ECHAM5-driven RegCM3 regional climate model deltas modifying the PRISM baseline (1), and averaged for two future time periods. Bottom row: Simulated ECHAM5-driven RegCM3 regional climate model differences between historical (1968–1999) and future (2015–2030; 2045–2060) average annual precipitation. For the difference maps, brown color tones represent drier conditions and blue colors represent wetter conditions. Note: There was a large bias in the RegCM3 simulations of historical precipitation for this region. Consequently, the climate model results were bias corrected to provide more realistic climate input to the vegetation model. Future climate projections (top row 2-3) were generated by calculating the ratios between future and historical precipitation values simulated by RegCM3 and multiplying them by the historical PRISM baseline.

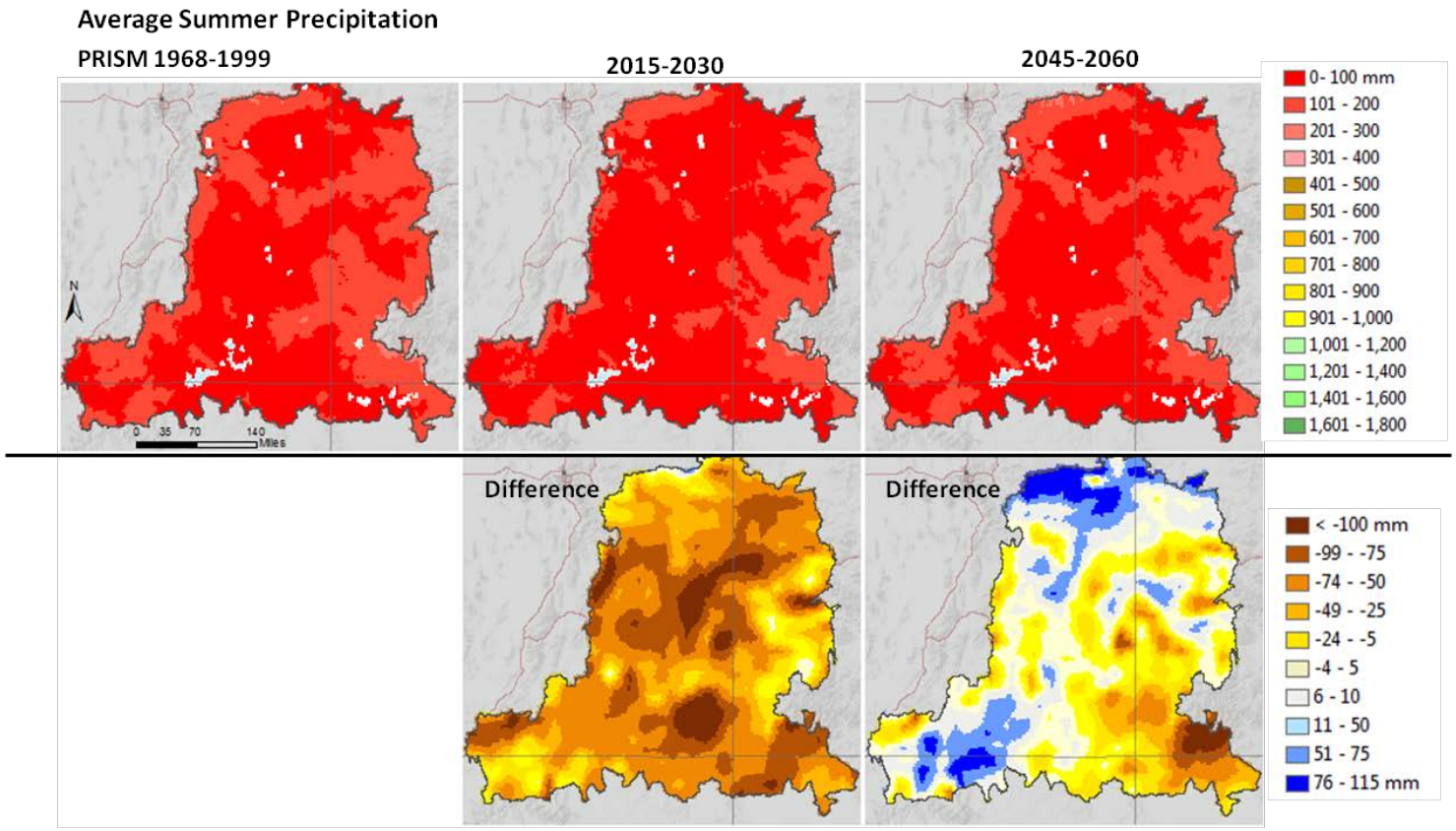


Figure 5-26. Map results for change in average annual summer precipitation. Top Row: 1) Observed summer precipitation (July–September) from PRISM averaged over the historical period (1968–1999 baseline) for the Colorado Plateau ecoregion.; 2-3) Bias-corrected future precipitation using the ECHAM5-driven RegCM3 regional climate model deltas modifying the PRISM baseline (1), and averaged for two future time periods. Bottom row: Simulated ECHAM5-driven RegCM3 regional climate model differences between historical (1968–1999) and future (2015–2030; 2045–2060) average summer precipitation. In difference maps, brown colors represent drier conditions and blue colors represent wetter conditions. Note: There was a large bias in the RegCM3 simulations of historical precipitation for this region. Consequently, the climate model results were bias corrected to provide more realistic climate input to the vegetation model. Future climate projections (top row 2-3) were generated by calculating the ratios between future and historical precipitation values simulated by RegCM3 and multiplying them by the historical PRISM baseline.

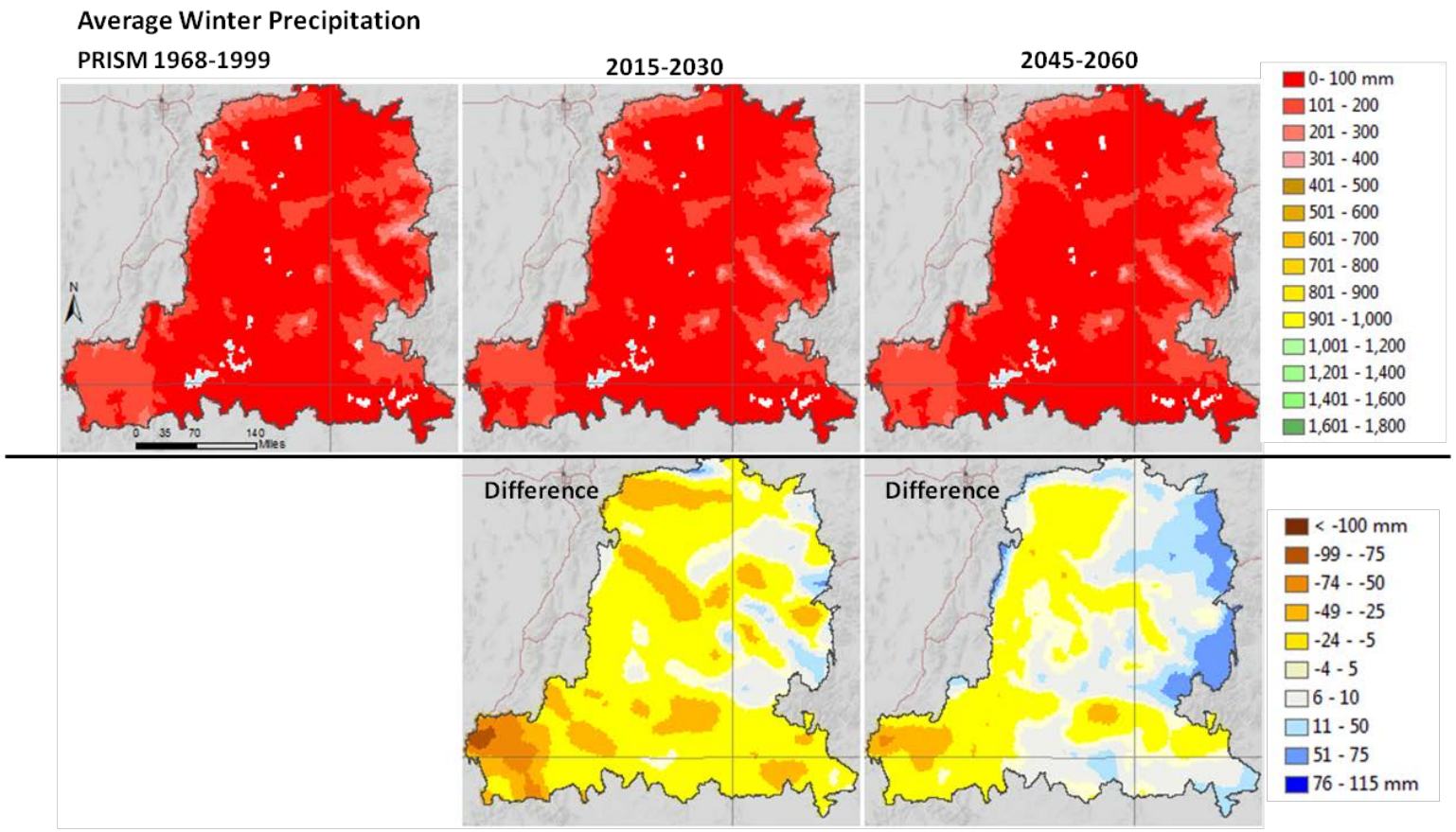


Figure 5-27. Map results for change in average annual winter precipitation. Top Row: 1) Observed winter precipitation (January–March) from PRISM averaged over the historical period (1968–1999 baseline) for the Colorado Plateau ecoregion.; 2-3) Bias-corrected future precipitation using the ECHAM5-driven RegCM3 regional climate model deltas modifying the PRISM baseline (1), and averaged for two future time periods. Bottom row: Simulated ECHAM5-driven RegCM3 regional climate model differences between historical (1968–1999) and future (2015–2030; 2045–2060) average winter precipitation. For the difference maps, brown color tones represent drier conditions and blue colors represent wetter conditions. Note: There was a large bias in the RegCM3 simulations of historical precipitation for this region. Consequently, the climate model results were bias corrected to provide more realistic climate input to the vegetation model. Future climate projections (top row 2-3) were generated by calculating the ratios between future and historical precipitation values simulated by RegCM3 and multiplying them by the historical PRISM baseline.

.

### *5.4.1.1 MAPSS Modeling Results*

Four different Mapped Atmosphere Plant Soil System (MAPSS) modeling outputs (see Chapter 3 Methods) were generated for the REA—Leaf Area Index (LAI), Potential Evapotranspiration (PET), Runoff, and Potential Vegetation distribution. Simulated LAI slightly declined overall in most areas, meaning that higher mortality causing canopy thinning or a shift to sparser, more drought-resistant vegetation may cause a change in vegetation communities in these locations (Figure 5-28). Only a few areas at higher elevations displayed any increase in LAI (green pixels on the difference maps). Changes in Potential Evapotranspiration (Figure 5-29) indicated an overall drying of the soil and, with the decline in LAI, suggested a probable decline in vegetation growth over most of the ecoregion (green areas on the map) with only a limited spattering of more moist conditions for vegetation (in purple, Figure 5-29). Runoff showed a slight decline over most of the ecoregion except for the eastern portion, which is expected to experience more runoff from higher elevations in the future (Figure 5-30).

One of the main projections from the MAPSS model is the potential shift in major vegetation types through time based on changes in plant functional groups. The model uses a historic climate baseline (PRISM) to predict the types of vegetation that would be supported under the given set of environmental conditions (see Methods, Climate Modeling, for more details). MAPSS does not take into account human management of natural landscapes (e.g. water management, logging, or grazing). It only uses the raw environmental variables (climate and soil) to predict vegetation. With a long history of human use in the ecoregion, the PRISM historic starting point should not be expected to reflect exactly what is on the ground today.

Considerable change in vegetation is predicted between 1968–1999 and 2045–2060 (Table 5-2 and Figures 5-31 and 5-32). Also, the MAPSS model is a static vegetation model that is run independently for each of the two time periods; therefore, one result does not affect the other. Normally, any dry or wet periods have repercussions on the following year's vegetation response. In this case, the static vegetation model just simulates what the instantaneous climate data can support.

The MAPSS model predicts that climate conditions will change to favor more grasses and shrubland subtropical xeromorphic (e.g., Gambel oak and western juniper). MAPSS results show small to moderate increases in $C_3$ grasses, tall and mid-sized $C_3C_4$ mixed grasses and larger increases in short $C_4$ and $C_3C_4$ mixed grasses (Table 5-2). Potential declines were reported in the vegetation communities shrub savanna evergreen, pinyon-juniper savanna continental, savanna evergreen needle continental, and forest evergreen needle continental. Munson et al. (2011), in a study examining historic climate-induced changes to vegetation plots in protected National Parks, predicted declines in $C_3$ grasses, no change in $C_4$ grasses, and increases in shrubs and woodland juniper. A partial explanation for the differences between the two results, particularly in the projection of the distribution of grasses, is that Munson et al. (2011) were looking at actual vegetation in parks that had experienced some human disturbance before the areas were protected and the MAPSS model focuses on projecting future potential vegetation reflecting no human influences and no community changes from agents such as invasive species.

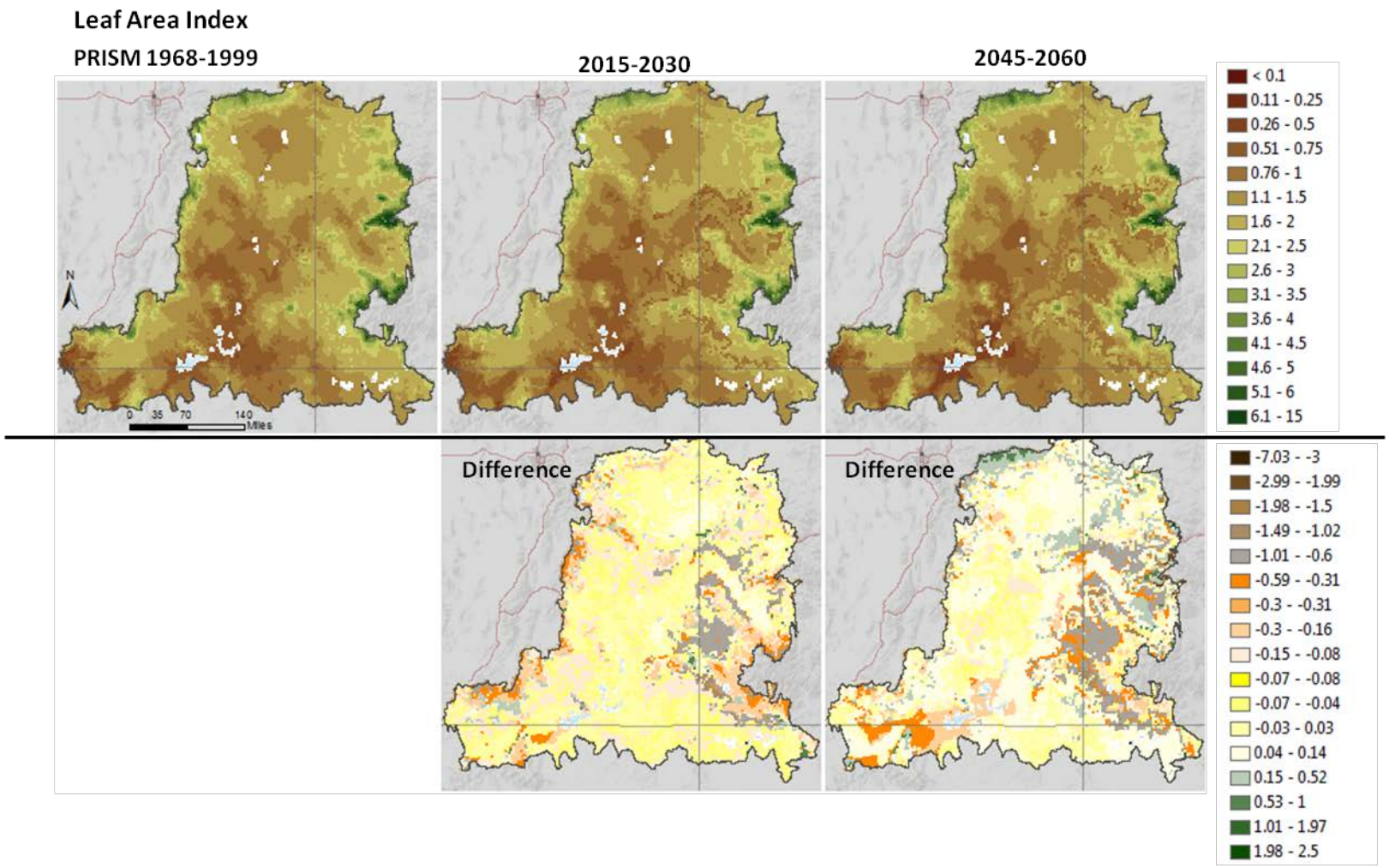


Figure 5-28. Map results for change in Leaf Area Index (LAI) based on MAPSS modeling for the Colorado Plateau ecoregion for 2015–2030 and 2045–2060.

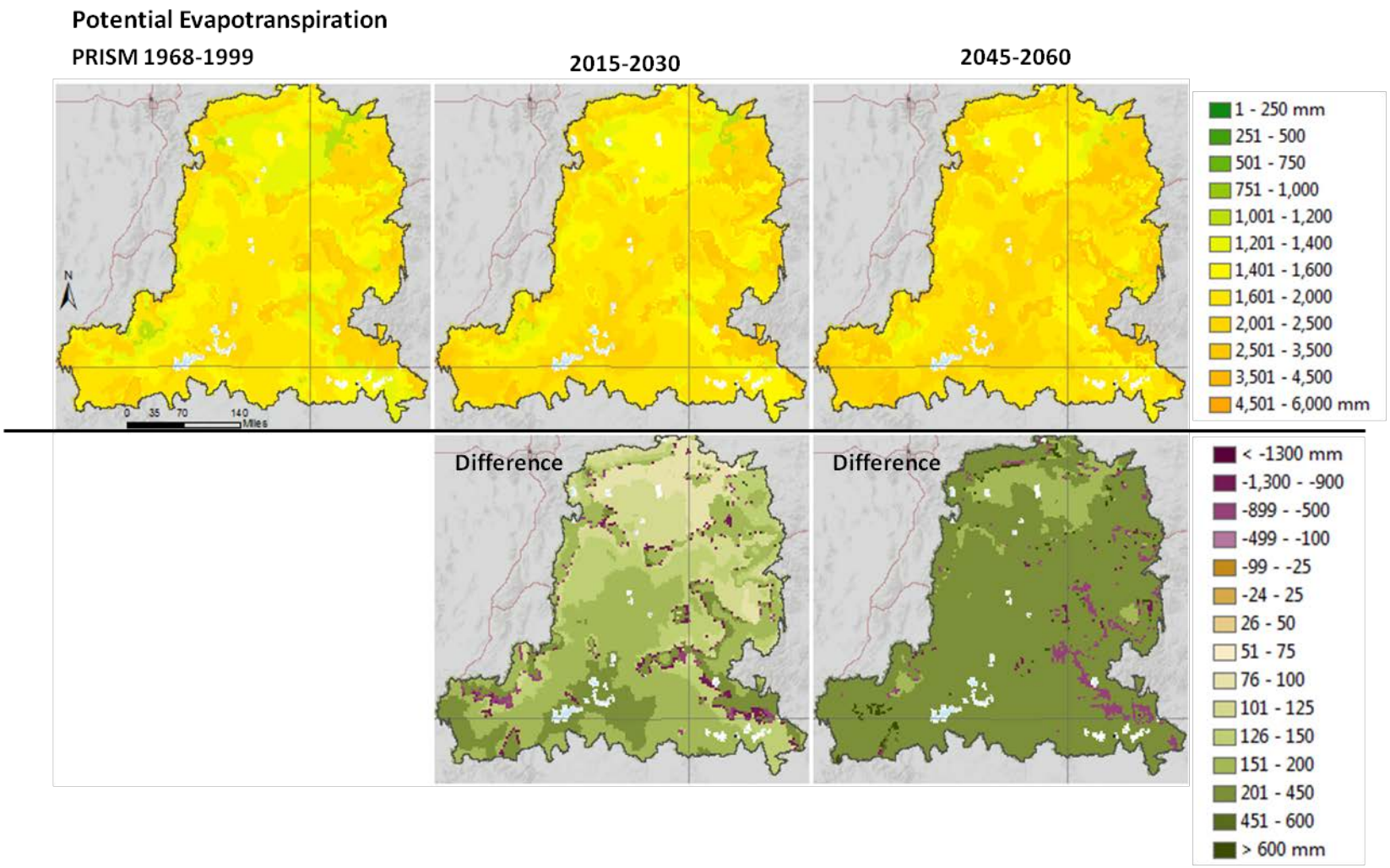


Figure 5-29. Map results for change in Potential Evapotranspiration (PET) based on MAPSS modeling for the Colorado Plateau ecoregion for 2015–2030 and 2045–2060.

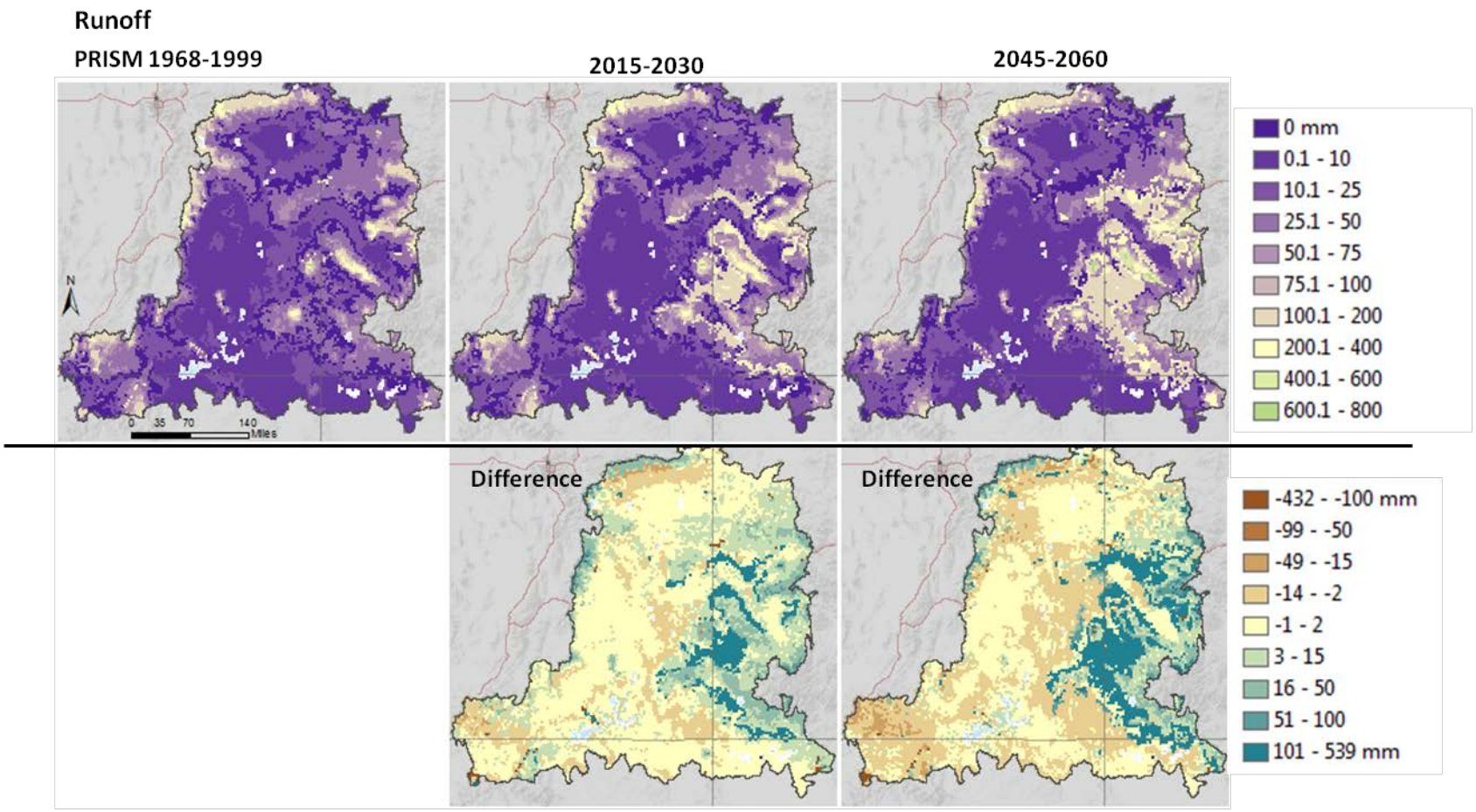


Figure 5-30. Map results for change in runoff based on MAPSS modeling for the Colorado Plateau ecoregion for 2015–2030 and 2045–2060.

Table 5-2. Change in major vegetation type (in 1000s of acres) according to MAPSS modeling for the Colorado Plateau ecoregion.

| PRISM | 2045–2060 | Potential Change | Vegetation Type | Example Species |
|---|---|---|---|---|
| 1,317 | 1,095 | -221 | Forest Evergreen Needle Continental | Douglas-fir, lodgepole pine |
| 0 | 71 | 71 | Tree Savanna Deciduous Broadleaf | Gambel oak |
| 5,844 | 5,353 | -490 | Tree Savanna Evergreen Needle Continental | ponderosa pine |
| 0 | 127 | 127 | Tree Savanna Mixed | mixed hardwoods, pines |
| 7,089 | 6,286 | -803 | Tree Savanna PJ Continental | pinyon pine, western juniper |
| 4 | 225 | 221 | Shrub Savanna Deciduous Broadleaf | blackbrush, greasewood, sagebrush |
| 29,593 | 22,319 | -7,275 | Shrub Savanna Evergreen | sagebrush, saltbrush |
| 1,139 | 2,432 | 1,293 | Shrubland Subtropical Xeromorphic | Gambel oak, western juniper |
| 43 | 134 | 91 | Shrubland Subtropical Mediterranean | mountain mahogany |
| 0 | 4 | 4 | Grass Tall C3 | Canada wildrye, needleandthread grass |
| 16 | 154 | 138 | Grass Mid C3 | bluebunch and thickspike wheatgrass, Indian ricegrass |
| 4 | 51 | 47 | Grass Short C3 | Sandberg bluegrass |
| 0 | 12 | 12 | Grass Tall C3C4 | wheatgrass, spike dropseed |
| 28 | 162 | 134 | Grass Mid C3C4 | wheatgrass, ricegrass |
| 257 | 2,167 | 1,910 | Grass Short C3C4 | bluegrass, grama |
| 0 | 8 | 8 | Grass Mid C4 | sideoats grama, James' galleta |
| 158 | 4,290 | 4,132 | Grass Short C4 | sandhill muhly, blue grama |
| 482 | 1,091 | 609 | Grass Semi Desert C4 | blue grama |
| 20 | 12 | -8 | Desert Subtropical | creosotebush |

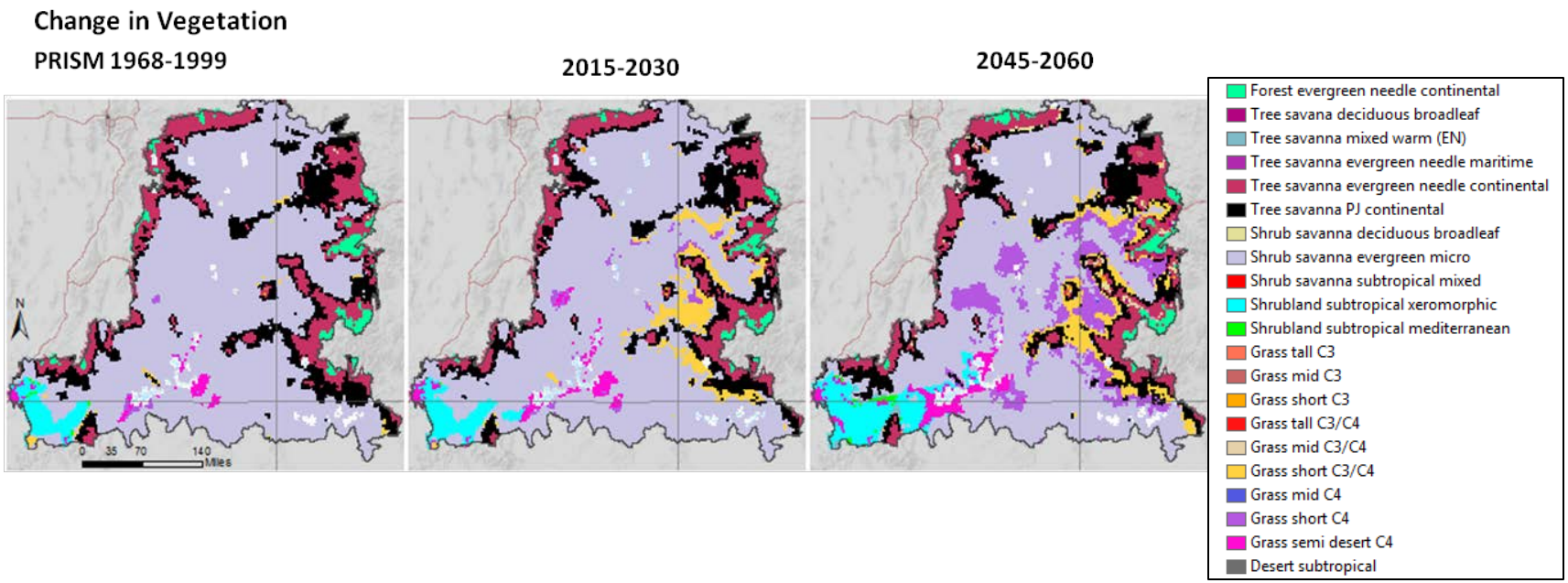


Figure 5-31. Map results for change in vegetation based on MAPSS modeling for the Colorado Plateau ecoregion from historic baseline (1968–1999) to 2015–2030 and 2045–2060.

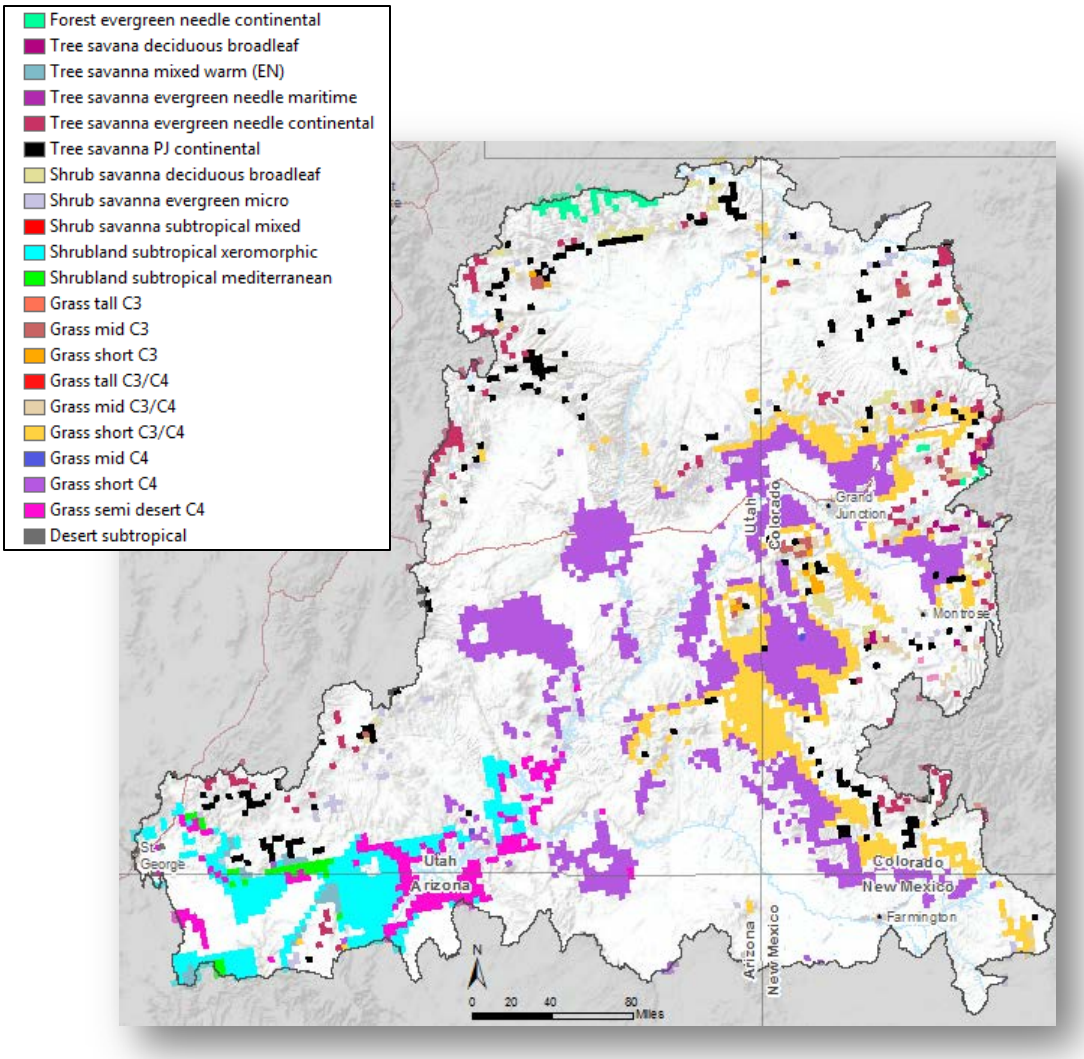


Figure 5-32. Map results showing just the pixels that changed to different vegetation types between historic baseline (1968–1999) and 2045–2060 based on MAPSS modeling for the Colorado Plateau ecoregion.

Potential vegetation change depicted here is simulated using climatic and soil information. The results do not mean the potential vegetation type will necessarily be established during a particular time period, only that climate conditions would be optimal for their development there at that time period if seed sources were available and human intervention did not occur to destabilize soils or modify its hydrological properties. Many other factors will affect future vegetation type such as human-caused fire, invasive species introduction, or dispersal factors. The projections may also indicate trends where vegetation mortality may occur.

The RegCM3 climate model projects increasing temperatures in all seasons and for both time scenarios. For 2015–2030, the model shows less precipitation annually, in winter and especially in summer (reduction in the monsoon); for 2045–2060, the model shows a slight increase in annual precipitation particularly during winter months. Regional differences can be found such as an increase in summer (monsoonal) precipitation in Utah and an increase in winter precipitation in Colorado. Winter precipitation is critical to perennial native plants and biological soil crusts and it enhances annual productivity especially for $C_3$ plants. If both winter and summer precipitation is reduced, trees, especially pinyon pine and biological soil crusts may be the biggest losers in this century (Schwinning et al 2008) while shrubs (e.g. blackbrush) are likely to continue to expand (Munson et al 2011).

The extremely warm and dry period in 2015–2030 may exacerbate the decline of native $C_3$ perennial grasses (Munson et al, 2011) and cause some tree mortality in many areas while favoring semidesert grasses in Western Colorado. By 2060 the model's big losers are some of the drier shrublands (sagebrush in particular), savanna pinyon-juniper, and some evergreen forest. Gains are expected in the grasses, especially short $C_4$ and short $C_3C_4$ mixes. Elevated $CO_2$ is expected to slightly favor $C_3$ over $C_4$ plants, which are less sensitive to warmer temperatures, and thus the increased projections in $CO_2$ may mitigate some of the effects of projected warming on the competitive advantage of $C_4$ grasses. This was confirmed in a recent experiment with $C_3$ and $C_4$ semi-arid steppe grasses (Morgan et al. 2011). Morgan et al. (2011) found that elevated $CO_2$ favored $C_3$ grasses and warming favored $C_4$ grasses. They also noted that the *combination* of warming and $CO_2$ enrichment stimulated the growth of $C_4$ grasses. Their overall results indicated that productivity in semi-arid grasslands may be higher than previously projected under climate change scenarios.

For both the 2015–2030 and 2045–2050 time periods, the seasonality and intensity of precipitation will be a key factor. Biological soil crusts are vulnerable to an increased frequency of summer rains (Belnap et al. 2004). Summer rain creates short wet-dry cycles that result in carbon and nitrogen losses to soil crusts and that could cause increased mortality or extirpations of some crust species (Evans et al. 2001). If the trend is toward wetter winters or springs, the invasive $C_3$ grasses such as cheatgrass or red brome will spread and will burn in the summer and fall, reinforcing their persistence over larger areas. If multiple wet years occur, grasses may have the advantage over shrubs in establishment and survival (Peters 2011).

In summary, land managers should begin to prepare for changes in the present ecoregion character (and boundaries) that could be expressed as shifts in vegetation composition, diversity and growth, declines in net primary production, intensification of the hydrologic cycle (more intense runoff), reductions in streamflow, declines in native fish diversity, increases in soil erosion, increases in nonnative species populations, and increased frequency and intensity of fire (Archer et al, 2008).

### *5.4.1.2 Uncertainty*

Uncertainty can be examined in different ways and from different perspectives. First, impacts models depend on the reliability of the climate data that they use. It is important to note that while climate projections diverge after 2040, models generally agree for the first half of the century and the choice of a particular climate model or scenario is less important if the management goal is limited to the next 2 or 3 decades. Beyond 2040, it becomes critical to rely upon experts who can select climate models based on less than perfect criteria. For example, it is common to choose climate models that best simulate past climate dynamics, particularly paying attention to the most important local climate feature (as was done for this REA with the choice of the RegCM3 model that recognizes the summer monsoon for the U.S. Southwest). Three GCMs driven by the RegCM3 regional model were analyzed for this project: ECHAM-5, GFDL and GENMOM. The data portal contains the results of each model, including associated MAPSS results. Users can delve into these models to gain a deeper understanding of the range of potential results from various models.

Model verification is obviously impossible for future projections and one is reduced to putting one's confidence in the ability of climate models to reproduce faithfully past climatic changes. However, there is no guarantee that a model that reproduces the past well will simulate the future accurately. Current models include our current understanding of past climate dynamics that may change drastically as atmospheric and stratospheric composition change as well as the planet's albedo. General circulation models (GCMs) were designed to simulate the planet's climate and their results compare well to climate observations at the global scale. The accuracy of global models declines at the local scale due to their inherent coarse spatial resolution that averages diverse vegetation cover and complex topography so important to conservation practitioners. Downscaling techniques (statistical or dynamic) bring GCM results to the scale of concern, but their accuracy is limited to that of the original projection. Furthermore, feedbacks from the biosphere to the atmosphere continue to be woefully under-represented in global models and regional model feedbacks to the GCMs have not even been developed yet. The uncertainty of climate projections result from the imperfect knowledge of 1) initial conditions such as sea surface temperatures that are difficult to measure, 2) the levels of future anthropogenic emissions which are unknowable since they are dependent on current and future political decisions and social choices and not on physical laws of nature, and finally 3) general system behavior (such as clouds, ice sheet melt) that continues to be the subject of basic climate research and that constitutes the "known unknowns" of the climate system. Finally, while surprises have been projected for the biological world, as the climate is changing, surprises such as the unexpected Larsen B ice shelf rapid collapse, the "unknown unknowns", also bring climate scientists back to the drawing board to improve existing models. It is important to understand that as change occurs (e.g. ice free poles, glaciers disappearance, new wind patterns, change in ocean currents), the basic assumptions at the core of the climate models may become obsolete, reminding us again that there is no assurance that a model that reproduces the past well is going to be reliable when projecting the future. Climate scientists learn constantly from every new observation and they update their models accordingly as new observations bring new knowledge.

Extreme events (e.g. long, intense droughts, flood, hurricanes or typhoons) are also difficult to predict by general circulation models. The 2007 report from the IPCC warns about the increased risk of more intense, more frequent and longer-lasting heat waves as exemplified by the European heat wave of 2003 that killed several thousand people. Along with a greater risk of drought, there is an increased chance of intense precipitation and flooding due to the greater water-holding capacity of a warmer atmosphere such that both wet and dry extremes should become more severe. These extreme events, while unpredictable, are often what shape our landscapes. Past extreme events such as the drought of the 1930s that caused the Dust Bowl in the USA certainly affected natural ecosystems and human land use. Recently, records of extreme events have been increasing. For example, the drought of 1999–2002 that spawned fires, dust storms, and pinyon pine mortality across the southwestern states may have been an indication of climate destabilization. A

drought in the summer of 2010 that caused crop failure and huge fires in Russia occurred at the same time as record rainfall that caused extensive flooding and loss of lives in both China and Pakistan. These extremes are consistent with what climate scientists have been expecting. Extreme events certainly pose a challenge to land managers who are typically more comfortable thinking about chronic linear change rather than abrupt and unpredictable change. Yet these events should be considered when trying to prepare for change. In the past, the reliability of models was tested in part by simulating large disturbances and observing the simulated system's response. It may be of interest to practitioners to focus now more on disturbance simulation to fully explore the resilience of their system.

There is also inherent natural variability in the expression of climate (e.g. cold air drainage, inversions in deep valleys), which is often influenced by the complexity of the regional terrain. At a fine scale, this means localized climate refugia–narrow swales, moist draws, etc. Close examination of a reasonable resolution (30 m) digital elevation model (DEM) can provide some insight as to locations that are more likely to provide refugia (Figure 5-33). These sites are found at a much finer scale than the analytical grid of the climate change work. At a coarser level, places on the landscape in and around rugged terrain will experience higher natural levels of climate variability.

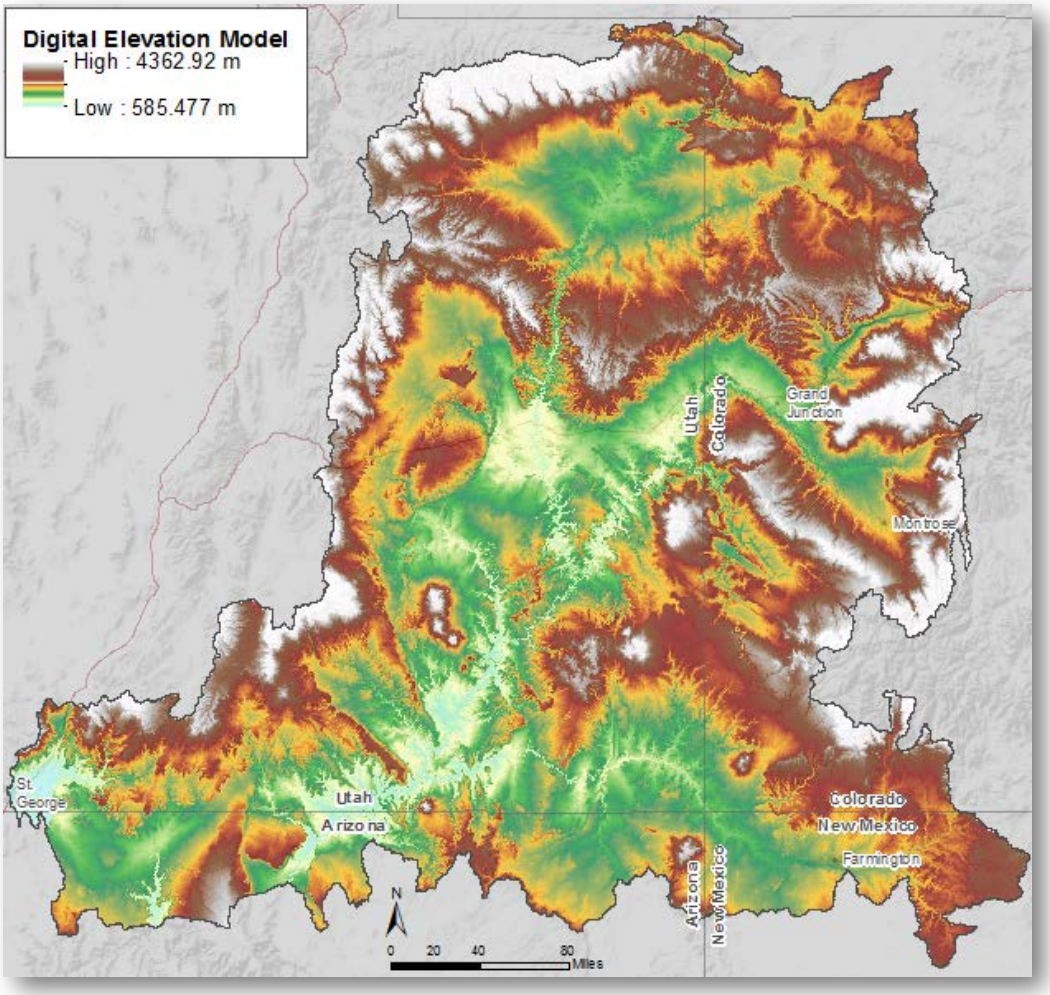


Figure 5-33. Digital elevation model (DEM) for the Colorado Plateau ecoregion.

Calculating the pixel standard deviation of annual average temperature and annual average precipitation separately based on the PRISM historic climate data provides map products that highlight areas on the landscape that are prone to more variability for these primary climate variables (Figure 5-34). The natural variability of precipitation for this arid landscape is quite small at lower elevations, but the range of variability increases to a modest degree as elevation increases. The range of variability is far more pronounced for the temperature data. Here, the valleys express higher levels of temperature variability from year-to-year (areas that are orange). These areas are highly influenced by the close proximity of the various mountains and benches. These results allow us to state two things. First, plants and animals living in areas that are more naturally variable in their climate have evolved mechanisms to help cope in that setting. It also suggests that the climate forecasts in these areas will tend to be less reliable compared to other locations in the region.

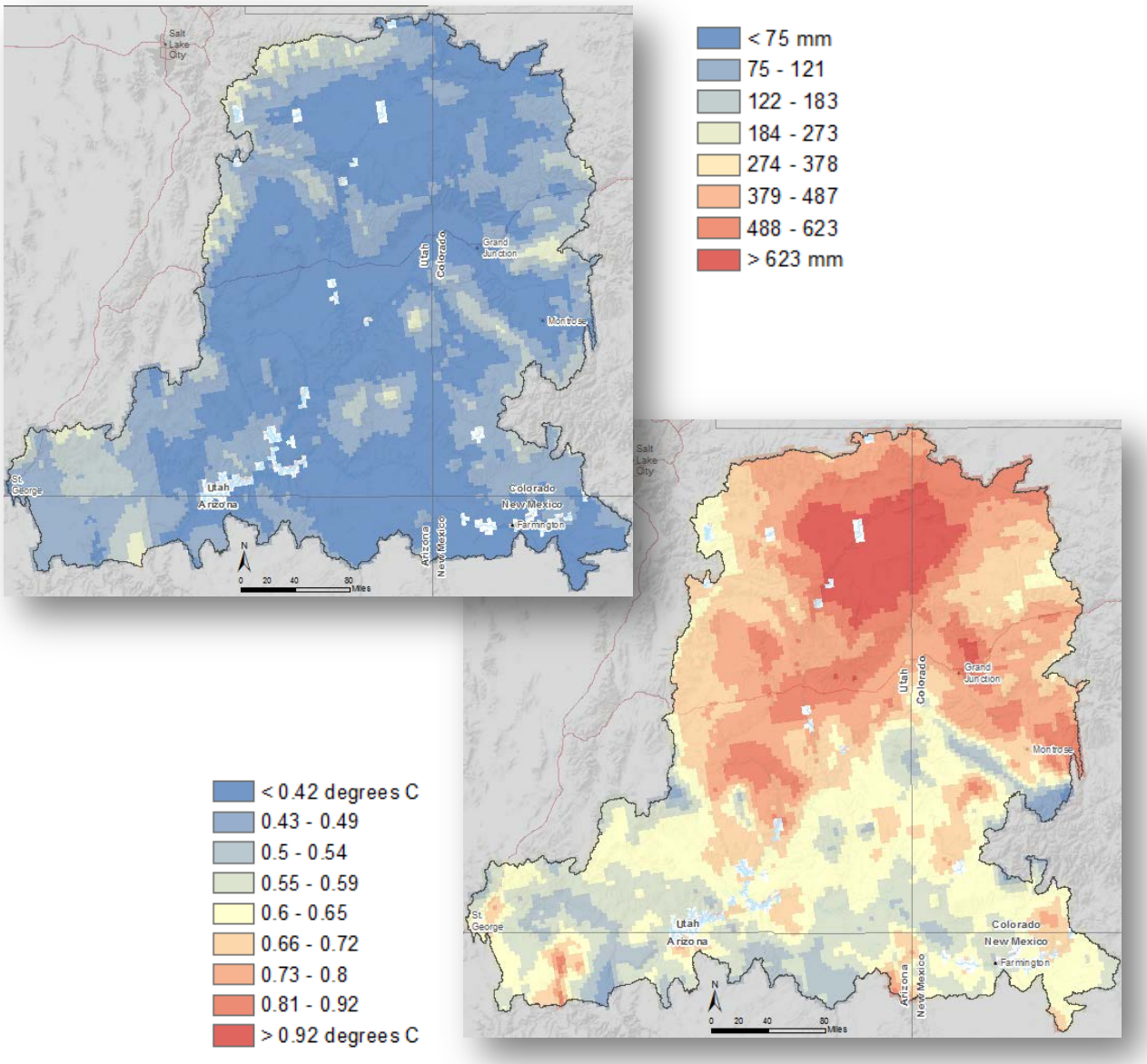


Figure 5-34. Uncertainty depicted as standard deviation of precipitation (A) and temperature (B) data from PRISM historic conditon (1968–1999).

### *5.4.1.3 Assessing Conservation Elements' Exposure to Climate Change*

To simplify the numerous future climate projections and MAPSS modeling results, a number of key findings from these analyses were selected and assembled into an overall relative climate change map. The different classes of potential for climate change were then overlaid on the distributions of specific conservation elements to assess the relative impact. The fuzzy model inputs included potential for summer temperature change and potential for winter temperature change averaged into a single factor, potential for runoff change from MAPSS modeling, potential for precipitation change, and potential for vegetation change again from MAPSS modeling (Figure 5-35). For this purpose the, direction of the change was not important—only degree of departure from historic measures. Details regarding change in temperature by degrees or actual predicted changes in precipitation can easily be assessed from the additional datasets provided in the body of the text or in the appendices. The model logic states that all 4km pixels with potential to change in primary vegetation type get the highest change score with the average of the other factors filling in the rest of the landscape.

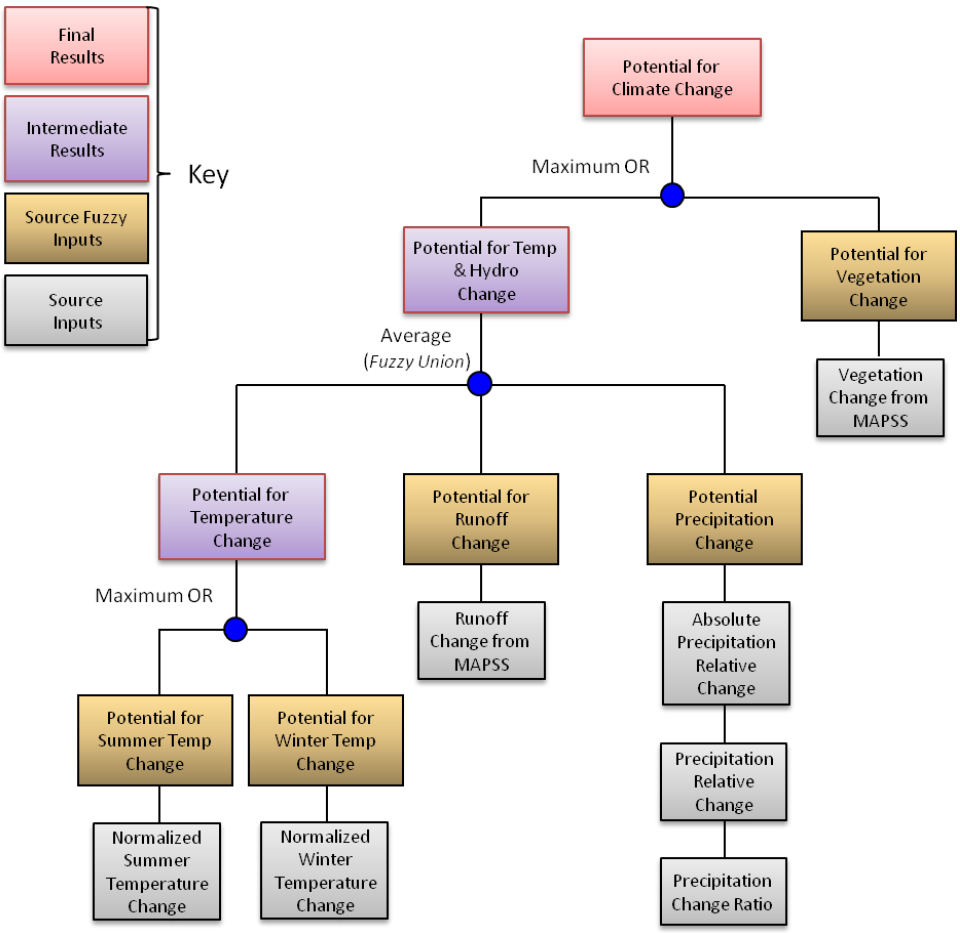


Figure 5-35. Fuzzy logic model for integrating climate change impacts to assess potential exposure of conservation elements to climate change.

Resultant maps from the fuzzy logic model show the contributions made by the various components **(**Figure 5-36). Areas likely to show the most change are those that either are predicted to change in their vegetation type or as a combination of all the other factors.

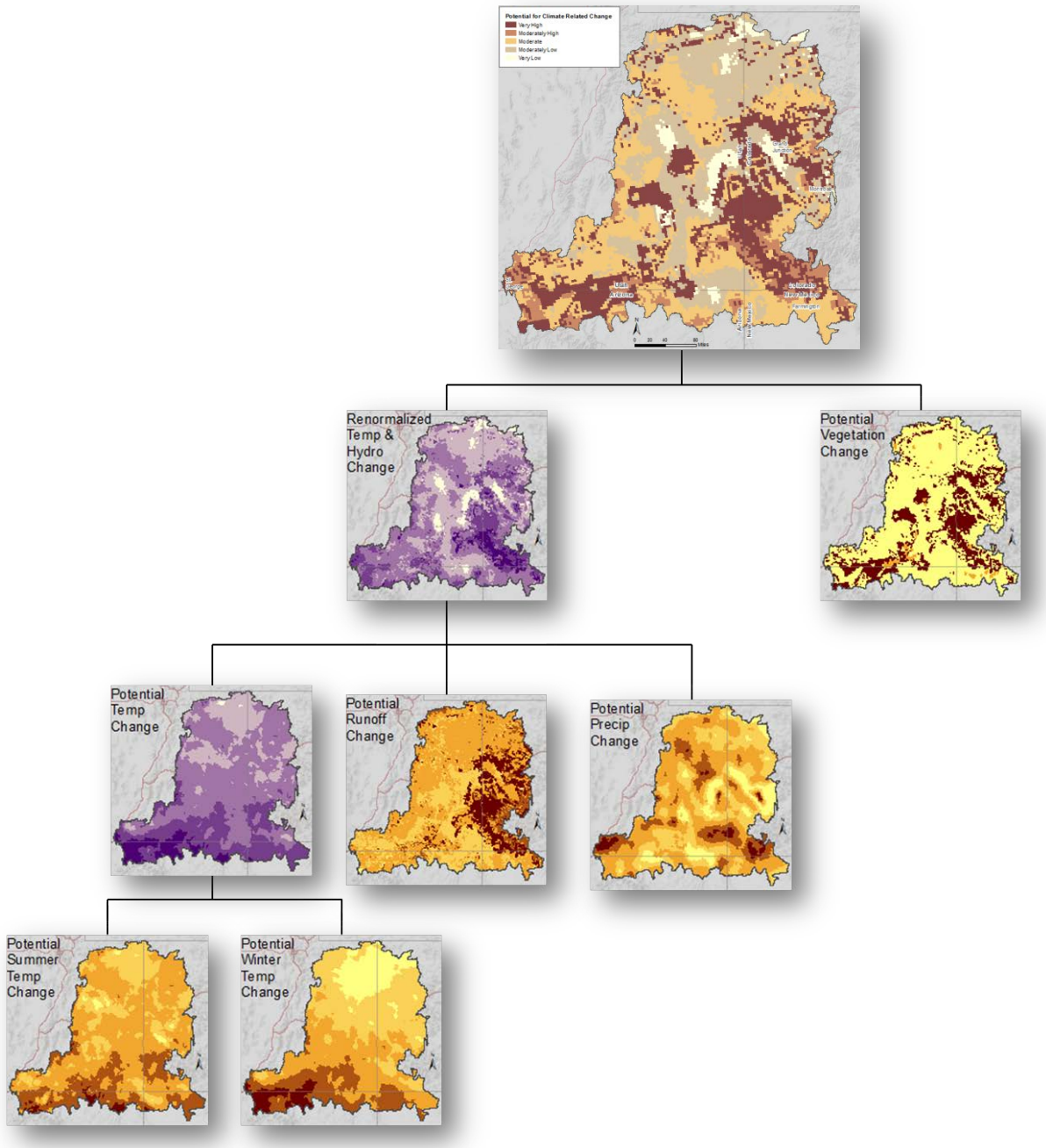


Figure 5-36. Map outputs for each step in the climate change fuzzy logic model for the Colorado Plateau ecoregion.

The climate change model results were then overlaid with species' and vegetation communities' distribution maps to assess their exposure to climate change. Exposure is just one aspect of ecosystem and species' vulnerability to climate change. Vulnerability is defined by the United Nations' Intergovernmental Panel on Climate Change (IPCC 2001) as…"(t)he degree to which a system is susceptible to, or unable to cope with, adverse effects of climate change, including climate variability and extremes. Vulnerability is a function of the character, magnitude, and rate of climate variation to which a system is exposed, [*as well as*] its sensitivity and its adaptive capacity." See also definition in Glick et al. (2011). The sensitivity of a species or system to climate change can be considered in terms of a "dose-response" relationship describing its exposure, resulting impacts, and its response (decline or adaptation, Füssel and Klein 2006). The development of vulnerability indices requires the implementation of species-specific indicators of sensitivity and species response or capacity to adapt, along with thresholds of impact that may lead to species decline (Carter et al. 2007). Füssel (2007) notes that time must be factored in as well; sensitivity represents immediate or short-term effects on a system or species, while resilience or adaptation must be considered over a longer time frame to assess or project the species' ability to maintain basic functions and possibly return to its original state. Although no readily-available metrics yet exist to quantitatively describe the vulnerability of an ecosystem or species to climate change (Füssel and Klein 2006, Adger 2006, Carter et al. 2007), the pressing need to identify vulnerable species and to manage for mitigation under various climate change scenarios has prompted the development of more qualitative approaches to project species' vulnerability (Glick et al. 2011, Young et al. 2011).

The REA climate change results presented here are modeled from available spatial data and focus mostly on exposure. However, some non-spatial sensitivity information was also available for many of the REA wildlife and vegetation community conservation elements from a Climate Change Vulnerability Index (CCVI) developed for the Nevada/Mojave region and the Gunnison Basin in western Colorado (NNHP 2011, TNC 2011). CCVI is a product of assessment teams employing literature review, professional judgment, and expert review through workshops (Young et al. 2011). All of the REA wildlife species conservation elements were classified in the two available CCVIs as *Presumed Stable*, except for Gunnison sage-grouse, greater sage-grouse, and Colorado River cutthroat trout, all of which were listed as *Highly Vulnerable* to significant decreases in abundance or distribution with projected climate change (NNHP 2011, TNC 2011). Razorback sucker was in the class *Increase Likely* within the Nevada/Mojave region. Five of our REA species were not listed: mountain lion, white-tailed prairie dog, black-footed ferret, pronghorn, and Mexican spotted owl. Vegetation communities were assessed only for the Gunnison Basin (of which the lower portions through the pinyon-juniper community occur within the Colorado Plateau ecoregion); of these, montane sage is in the category *Moderately Increase* and the big sage and pinyon-juniper communities are in the *Presumed Stable to Moderately Increase* categories (TNC 2011).

For the body of this report, results were posted in histograms as five climate change exposure classes for 2060: Very High, High, Moderate, Moderately Low and Low for the potential for an area to be affected by climate change as defined in the fuzzy logic model. One can portray this aspect of potential vulnerability (exposure) by overlaying the conservation element's distribution map (Section 4.2) with the climate change exposure map (top map in Figure 5-36). An overlay map for each conservation element relative to climate change exposure can be found in Appendices B and C; the maps and data may also be examined in greater detail on the data portal (access at http://www.blm.gov/wo/st/en/prog/more/climatechange.html). Bringing additional species sensitivity information to this analysis, such as that for the Highly Vulnerable species listed above, will allow the identification of locations where the species may experience various degrees of vulnerability to climate change as well as locations of possible refugia.

Each of the mammal species showed a unique signature to the climate model results (Figure 5-37). Gunnison's prairie dog showed the highest exposure of any of the mammals with 70% of its current distribution in the Very High category. The severely-limited black-footed ferret population scored low in

exposure; however, when considering its potential reintroduction, the profile for the white-tailed prairie dog is just as important; it showed somewhat greater potential impacts from both climate change and the potential for energy development discussed in Section 5.2. Desert bighorn sheep, inhabiting somewhat higher elevations, is in a lower exposure category. Mountain lion and two prey species (especially mule deer) showed similar potential exposure with about a third of their populations under Very High or High climate change conditions.

Figure 5-37. Potential exposure to climate change for mammals of the Colorado Plateau ecoregion. Note: Percent distribution (y-axis) differs for each species. Gunnison's prairie dog showed the highest exposure of any of the mammals with 70% of its current distribution in the Very High category.

The bird species also showed species-specific patterns (Figure 5-38). Gunnison sage-grouse, like its prairie dog companion, is the species with the highest exposure with about 70% of its current distribution affected by climate change by 2060. Yellow-breasted chat, a riparian species, also showed high exposure to changing climate in the region. Greater sage-grouse, on the other hand, showed a very different pattern with most of its current populations in the lower exposure classes. Mexican spotted owl fared better than the remaining bird species, and all of the others shared a similar profile expressing only subtle differences. Like the mammals, around a third of the distributions for these species are predicted to be under Very High or High climate change exposure in the mid-term future.

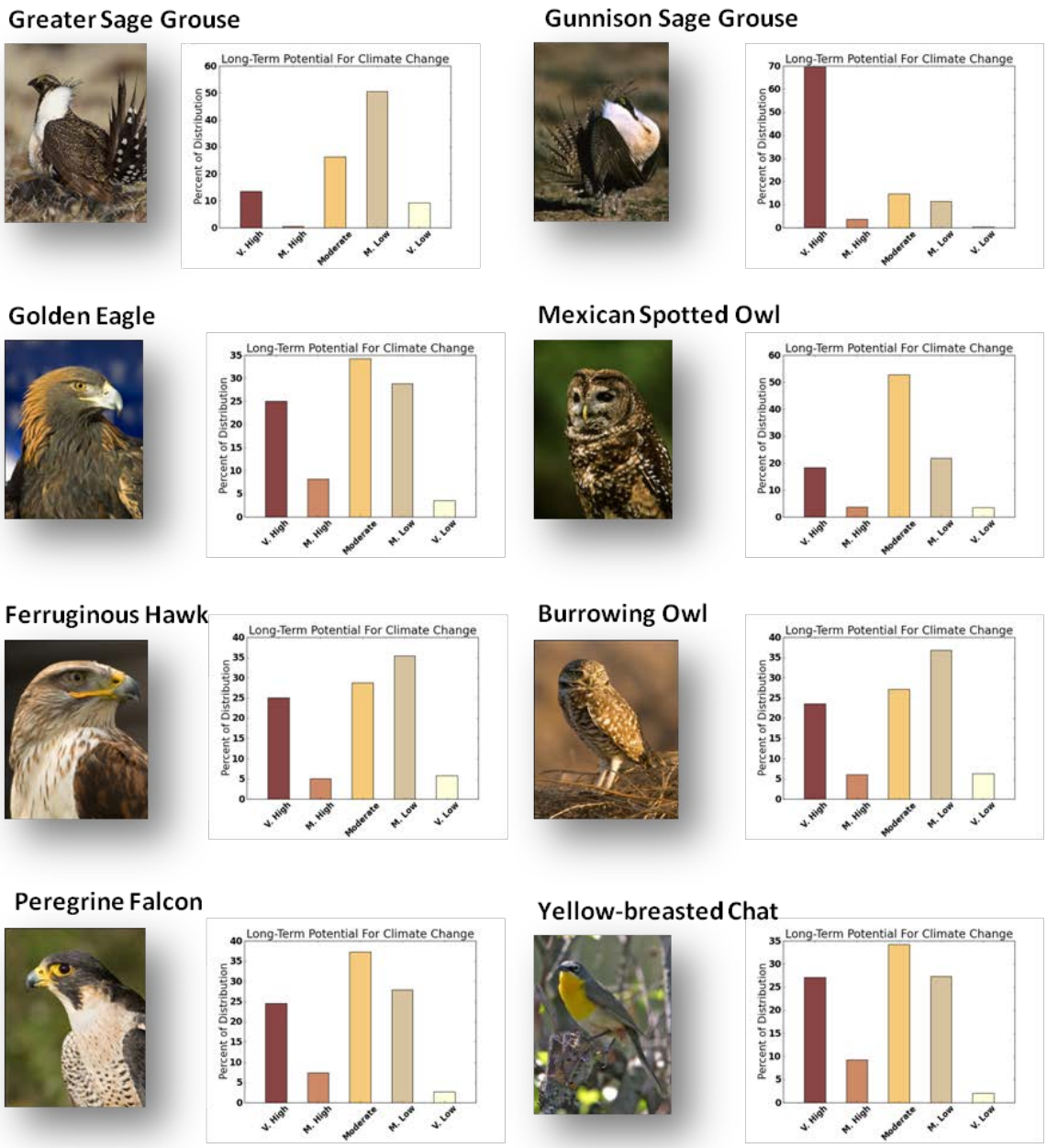


Figure 5-38. Potential exposure to climate change for birds of the Colorado Plateau ecoregion. Note: Percent distribution (y-axis) differs for each species.

Of the fish species, flannelmouth sucker showed the highest exposure from climate change compared to the other two species (Figure 5-39). Colorado River cutthroat trout experienced somewhat less exposure than flannelmouth sucker with almost 30% in the Very High and Moderately High classes. Wenger et al. (2011), using a composite model of multiple climate projections, found a decline in stream length with suitable habitat for Colorado cutthroat of 28% in the 2040s and 58% in a 2080s scenario from a combination of temperature increases and interactions with other introduced trout species. The authors estimate that interactions with introduced species decrease current cutthroat stream length by 33% and future 2080s scenario stream length by 26%. See more details on fish species in Appendix C.

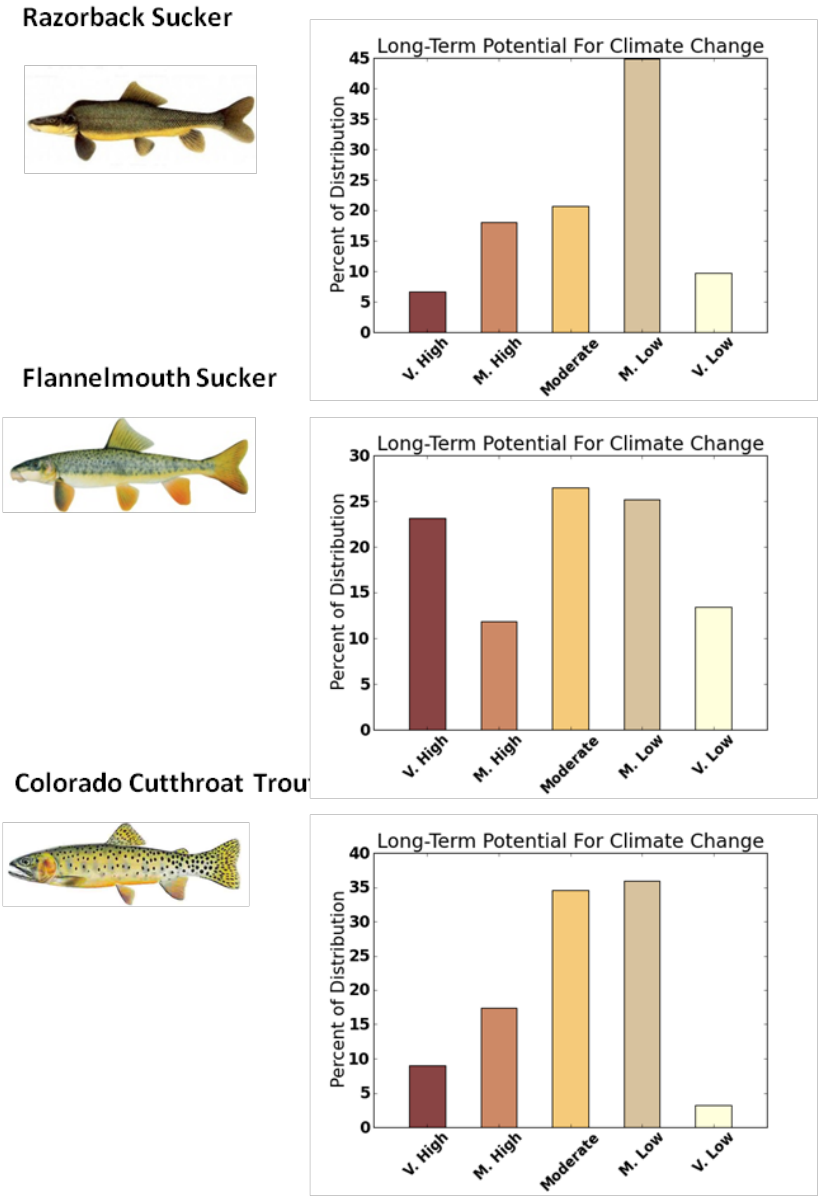


Figure 5-39. Histograms show potential exposure to climate change for the fishes of the Colorado Plateau ecoregion. Of the fish species, flannelmouth sucker showed the highest potential exposure to climate change compared to the other two species.

The vegetation communities (Figure 5-40) showing the most area under high climate change exposure include the shrublands (especially big sagebrush and blackbrush-Mormon-tea communities), riparian vegetation, and pinyon-juniper woodland, which is consistent with the MAPSS results presented in Table 5-2. With the vegetation communities, note that when interpreting these results high exposure does not definitively mean decline; it means higher probability of change. Insects and disease will play a collateral role with the effects of climate change in altering the dominance and distribution of various vegetation species.

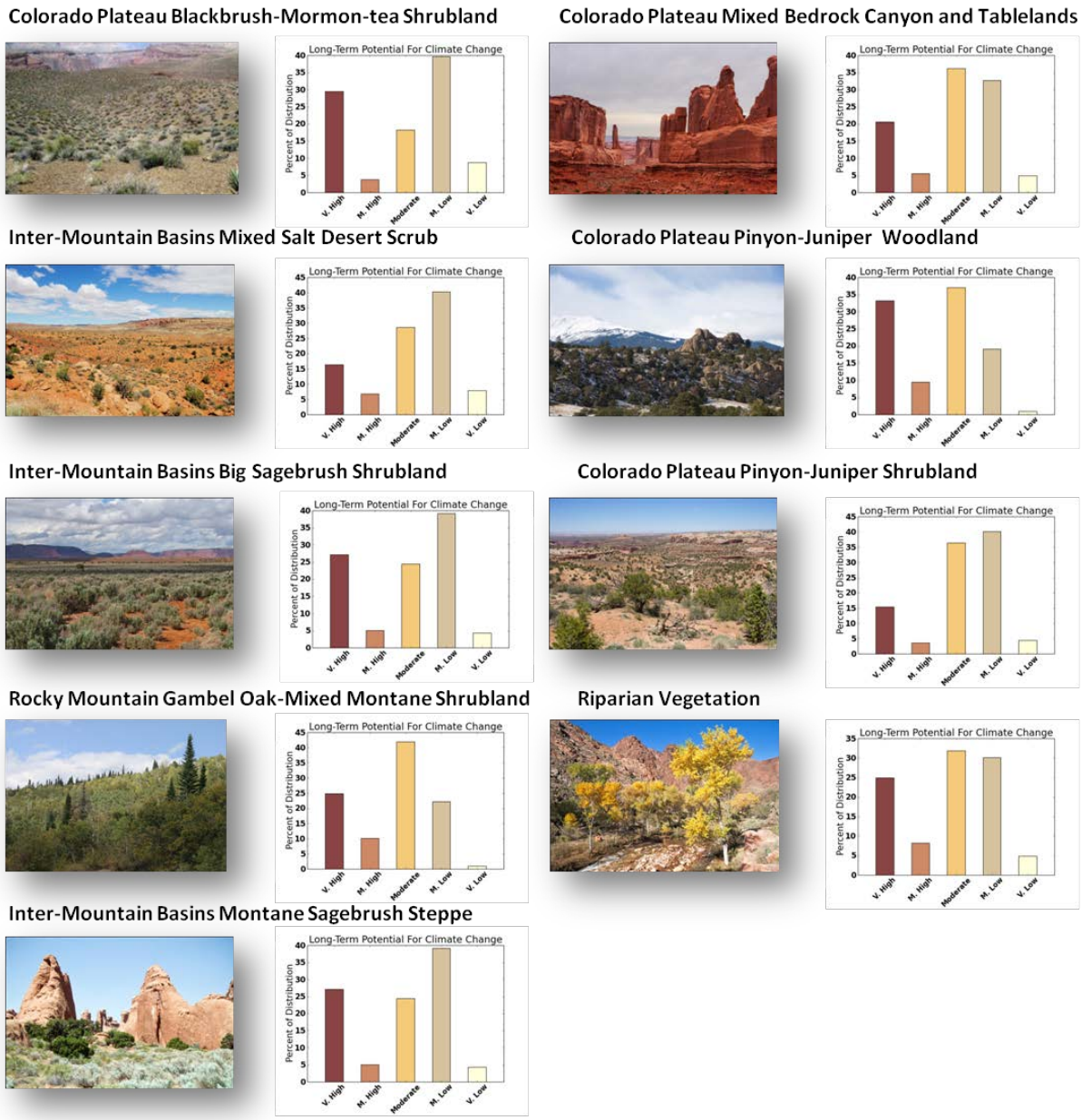


Figure 5-40. Histograms show potential exposure to climate change for the vegetation communities of the Colorado Plateau ecoregion. The big sagebrush and blackbrush-Mormon-tea communities show the most area under high climate change exposure in addition to riparian vegetation and pinyon-juniper woodland, which is consistent with the MAPSS results presented in Table 5-2.

Finally, existing designated sites show fairly high exposure to climate change by 2060 with 30% of land area under Very High or High and nearly another 40% under Moderate vulnerability (Figure 5-41).

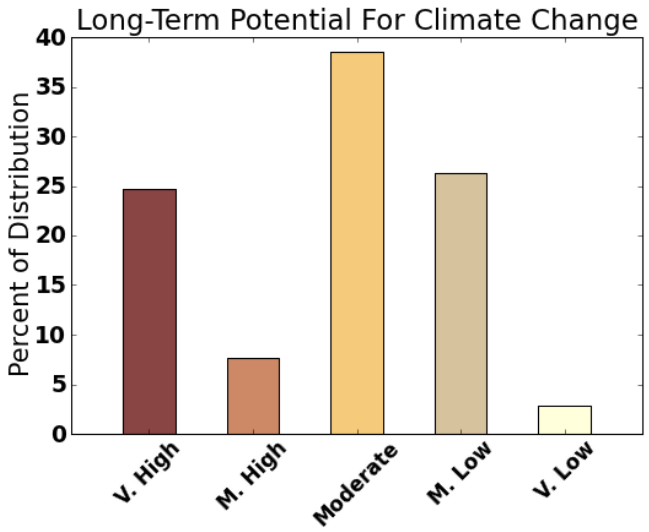


Figure 5-41 Potential exposure to climate change for the designated sites of the Colorado Plateau ecoregion with 30% of land area under Very High or High and nearly another 40% under Moderate potential for climate change.

## 5.5 References Cited


Adger, W.N. 2006. Vulnerability. *Global Environmental Change* 16(3): 268–281.

Archer, S.A. and K.I. Predick. 2008. Climate change and ecosystems of the Southwestern United States. *Rangelands* 30(3): 23-38.

Belnap, J., S. L. Phillips and M. E. Miller (2004). Response of desert biological soil crusts to alterations in precipitation frequency. *Oecologia* 141(2): 306-316.

Carter, T.R., R.N. Jones, X. Lu, S. Bhadwal, C. Conde, L.O. Mearns, B.C. O'Neill, M.D.A. Rounsevell, and M.B. Zurek. 2007. New assessment methods and the characterisation of future conditions. Pages 133–171 *in* Parry, M.L., O.F. Canziani, J.P. Palutikof, P.J. van der Linden, and C.E. Hanson (eds.), Climate change 2007: Impacts, adaptation and vulnerability, Contribution of Working Group II to the Fourth Assessment Report of the Intergovernmental Panel on Climate Change, Cambridge University Press, Cambridge, United Kingdom.

Copeland, H.E., K.E. Doherty, D.E. Naugle, A. Pocewicz, and J.M. Kiesecker. 2009. Mapping oil and gas development potential in the US intermountain west and estimating impacts to species. PLoS ONE 4(10): e7400.

Doherty, K. 2008. Sage-grouse and energy development: Integrating science with conservation planning to reduce impacts. PhD dissertation, University of Montana, Missoula. 125 pp.

Evans, R.D., J. Belnap, F. Garcia-Pichel, and S.L. Phillips. 2001. Global change and the future of biological soil crusts. Pages 417–429 *in* Belnap, J., and O.L. Lange (eds.), Biological soil crust: Structure, function, and management. Springer, New York.

Füssel, H.M. 2007. Vulnerability: A generally applicable conceptual framework for climate change research. *Global Environmental Change* 17:155–167.

Füssel, H.M., and R.J.T. Klein. 2006. Climate change vulnerability assessments: An evolution of conceptual thinking. *Climatic Change* 75 (3):301–329.

Garfin, G., J. Eischeid, M. Lenart, K. Cole, K. Ironside, and N. Cobb. 2010. Downscaling climate projections to model ecological change on topographically diverse landscapes of the arid southwestern United States. Pages 21–44 *in* Van Riper, C., III, B.F. Wakeling, and T.D. Sisk (eds.), The Colorado Plateau IV, Proceedings of the 9th Biennial Conference on Colorado Plateau Research, October, 2007. University of Arizona Press, Tucson.

Glick, P., B.A. Stein, and N.A. Edelson. 2011. Scanning the conservation horizon: A guide to climate change vulnerability assessment. National Wildlife Federation, Washington D.C.

Hostetler, S., J. Alder, and A. Allan. 2011. Dynamically downscaled climate simulations over North America: Methods, evaluation, and supporting documentation for users. Open-File Report 2011–1238, U.S. Geological Survey, Reston, Virginia.

IPCC (Intergovernmental Panel on Climate Change). 2001. Climate change 2001: Synthesis report. A Contribution of Working Groups I, II, and III to the Third Assessment Report of the Intergovernmental Panel on Climate Change. Cambridge University Press, Cambridge, United Kingdom.

Jarnevich, C.S., P. Evangelista, T.J. Stohlgren, and J. Morisette. 2011. Improving national-scale invasion maps: Tamarisk in the western United States. *Western North American Naturalist* 71(2):164–175.

Morgan, J.A., D.R. LeCain, E. Pendall, D.M. Blumenthal, B.A. Kimball, Y. Carrillo, D.G. Williams, J. Heisler-White, F.A. Dijkstra, and M. West. 2011. $C_4$ grasses prosper as carbon dioxide eliminates desiccation in warmed semi-arid grassland. *Nature* 476: 202–206.

Mote, P.W., D. Gavin, and A. Huyer. 2010. Climate change in Oregon's land and marine environments. Chapter 1 in Dello, K.D., and P.W. Mote (eds.), Oregon Climate Assessment Report. College of Oceanic and Atmospheric Sciences, Oregon State University, Corvallis, Oregon.

Munson, S., J. Belnap, C. Schelz, M. Moran, T. Carolin. 2011. On the brink of change: Plant responses to climate on the Colorado Plateau. *Ecosphere* 2(6), Article 68. digitalcommons.usu.edu/cgi/viewcontent.cgi?article=1340

NNHP (Nevada Natural Heritage Program). 2011. Climate Change Vulnerability Index (Release 2.01). Nevada Natural Heritage Program, Carson City, Nevada.

Peters, D.P.C., J. Yao, O.E. Sala, and J. Anderson. 2011. Directional climate change and potential reversal of desertification in arid and semiarid ecosystems. *Global Change Biology* (in press) DOI: 10.1111/j.1365-2486.2011.02498.x.

Schwinning, S., J. Belnap, D.R. Bowling, and J.R. Ehleringer. 2008. Sensitivity of the Colorado Plateau to change: Climate, ecosystems, and society. *Ecology and Society* 13(2): 28. http://www.ecologyandsociety.org/vol13/iss2/art28/

Seager, R., M. Ting, I. Held, Y. Kushnir, J. Lu, G. Vecchi, H. Huang, N. Harnik, A. Leetmann, N. Lau, C, Li, J. Velez, and N. Naik. 2007. Model projections of an imminent transition to a more arid climate in southwestern North America. *Science* 316:1181–1184.

TNC (The Nature Conservancy). 2011. Gunnison Basin preliminary climate vulnerability assessment for the Gunnison Climate Working Group. The Nature Conservancy, Southwest Climate Change Initiative, Colorado Natural Heritage Program, Fort Collins, Colorado.

Theobald, D.M. 2010. Estimating natural landscapes changes from 1992 to 2030 for the conterminous United States. *Landscape Ecology* 25(7):999–1011.

Van Dyke, F.G., R.H. Brocke, and H.G. Shaw. 1986. Use of road track counts as indices of mountain lion presence. *Journal of Wildlife Management* 50(1):102–109.

Wenger, S.J., D.J. Isaak, C.H. Luce, H.M. Neville, K.D. Fausch, J.B. Dunham, D.C. Dauwalter, M.K. Young, M.M. Elsner, B.E. Rieman, A.F. Hamlet, and J.E. Williams. 2011. Flow regime, temperature, and biotic interactions drive differential declines of trout species under climate change. *Proceedings of the National Academy of Sciences,* Published online before print August 15, 2011, doi: 10.1073/pnas.1103097108.

Young, B., E. Byers, K. Gravuer, K. Hall, G. Hammerson, and A. Redder. 2011. Guidelines for using the NatureServe Climate Change Vulnerability Index, Release 2.1. NatureServe, Arlington, VA.

P
h
Photo: Four Corners Powerplant from Lake Powell, National Park Service.